Evolutionary Games for Dynamic Network Resource Selection in RSMA-Enabled 6G Networks

Nguyen Thi Thanh Van, Nguyen Cong Luong, Shaohan Feng, Van-Dinh Nguyen, *Member, IEEE*, and Dong In Kim, *Fellow, IEEE*

***Abstract*— In this paper, we address a dynamic network resource selection problem for mobile users in a rate-splitting multiple access (RSMA)-enabled network by leveraging evolutionary games. Particularly, mobile users are able to locally and dynamically make their selection on orthogonal resource blocks (RBs), which are also considered as network resources (NRs), over time to achieve their desired utilities. Then, RSMA is used for each group of users selecting the same NR. With the use of RSMA, the main goal is to optimize the beamformers of the common and private messages for users in the same group to maximize their sum rate. The resulting problem is generally non-convex, and thus we develop a successive convex approximation (SCA)-based algorithm to efficiently solve it in an iterative fashion. To model the NR adaptation of users, we propose to use two evolutionary games, *i.e.* a traditional evolutionary game (TEG) and fractional evolutionary game (FEG). The FEG approach enables users to incorporate memory effects (*i.e.* their past experiences) for their decision-making, which is more realistic than the TEG approach. We then theoretically verify the existence of the equilibrium of the proposed game approaches. Simulation results are provided to validate their consistency with the theoretical analysis and merits of the proposed approaches. They also reveal that, compared with TEG, FEG enables users to leverage past information for their decision-making, resulting in less communication overhead, while still guaranteeing convergence.**

***Index Terms*— Dynamic network resource selection, evolutionary game, memory effect, orthogonal resource blocks, rate-splitting multiple access.**

I. Introduction

RATE-SPLITTING multiple access (RSMA) has been regarded as a promising technique for the next generation mobile networks (*i.e.* 6G) [1], [2], [3]. Following the RSMA principles, each original message intended to a user is split into common and private parts. The common parts of all users are combined into a single common message, while the private parts are encoded into separate messages (*i.e.* private messages) for the intended users [1]. Each user then recovers its original message from the decoded common and private messages. RSMA divides original messages into common and private parts to partially decode interference and partially treat interference as noise. Thus, RSMA enables flexible and powerful interference management to enhance the spectral efficiency, energy efficiency, reliability, and quality of service (QoS) compared with existing multiple access technologies such as space division multiple access (SDMA) and non-orthogonal multiple access (NOMA) [1], [2], [3], [4], [5]. Recently, several works related to RSMA have been investigated, and a comprehensive survey on RSMA can be found in [2]. In general, the works related to RSMA aim to maximize the sum rate, e.g., [6], [7], and [8], the minimum rate among users, e.g., [9] and [10], and energy efficiency, e.g., [4] and [11]. These objectives can be well obtained by optimizing the transmit power and beamformers associated with the common message and private messages.

However, the existing RSMA-related works have mostly considered a single subcarrier or single resource block (RB) where all users share the same subcarrier or the same RB. Different from the existing works, this paper investigates an RSMA-based cellular network with multiple orthogonal RBs. The proposed system is user-centric in which each user is allowed to dynamically select and access an RB over time. Thus, there may be multiple users competing for the access on the RB. Then, RSMA is used to allow multiple users to access the same NR. The main motivations are detailed as follows. First, RSMA allows the concurrent users to share the same spectrum through performing the power allocation to them. Thus, a base station (BS) may only support a limited number of users due to its limited power budget. To support more users, multiple RBs should be considered, and therefore, the proposed system includes the orthogonal multiple access (OMA) scheme. However, compared to OMA which allocates one RB to only one user, the proposed system can double the number of users by virtue of RSMA. Second, their respective channels associated with different RBs can be different from each other, which result in the difference in signal-to-interference-plus-noise ratio (SINR). Meanwhile, future networks are becoming user-centric that allow the users to locally and dynamically select and switch among network resources (NRs) over time to achieve their best QoS.

Manuscript received 21 July 2022; revised 15 October 2022; accepted 1 December 2022. Date of publication 30 January 2023; date of current version 18 April 2023. This work was supported in part by the National Research Foundation of Korea (NRF) Grant funded by the Korean Government (MSIT) under Grant 2021R1A2C2007638 and in part by the MSIT through ICT Creative Consilience Program supervised by IITP under Grant IITP-2020-0-01821. *(Corresponding author: Nguyen Cong Luong.)*

Nguyen Thi Thanh Van is with the Faculty of Electrical and Electronic Engineering, Phenikaa University, Hanoi 12116, Vietnam (e-mail: van.nguyenthithanh@phenikaa-uni.edu.vn).

Nguyen Cong Luong is with the Faculty of Computer Science, Phenikaa University, Hanoi 12116, Vietnam (e-mail: luong.nguyencong@phenikaa-uni.edu.vn).

Shaohan Feng is with the Institute for Infocomm Research, Singapore 138632 (e-mail: fengs@i2r.a-star.edu.sg).

Van-Dinh Nguyen is with the College of Engineering and Computer Science, VinUniversity, Hanoi 100000, Vietnam (e-mail: dinh.nv2@vinuni.edu.vn).

Dong In Kim is with the Department of Electrical and Computer Engineering, Sungkyunkwan University, Seoul 16419, South Korea (e-mail: dikim@skku.ac.kr).

Color versions of one or more figures in this article are available at https://doi.org/10.1109/JSAC.2023.3240779.

Digital Object Identifier 10.1109/JSAC.2023.3240779

This, on the other hand, reduces the complexity of resource allocation task at the BS since the task is partially done at user side. Therefore, a natural question that arises is how to model the dynamic RB selection of users while still guaranteeing the optimal system performance.

Evolutionary game has been considered as an effective tool to model the selection behavior of players [12]. That is, each player in the game is able to dynamically adjust its selection strategy until achieving a solution at which it has no an incentive to change its strategy since this will undermine other players' utility. The solution is known as the equilibrium of the game. The local decisions of users and the equilibrium are very crucial in the area of communication and networking that guarantee the long-term stability as well as scalability of the network. Therefore, evolutionary game has been widely adopted to study dynamic network service (e.g. 4G, 5G, wireless LAN) selection of mobile users [13], [14], [15], [16]. As presented in [14], the computation complexity of strategy adaptation at the user side is low (*i.e.* $\mathcal{O}(1)$) that is suitable in dynamic network environments.

The advantages of the evolutionary game motivate us to adopt this game for studying the dynamic RB selection of users in the RSMA-enabled networks. The major contributions of the paper are as follows:

- We consider a dynamic, i.e., time-variant, network resource selection problem in an RSMA-enabled cellular network. The considered network allows users to locally and dynamically select and adapt RBs over time to achieve their desired QoSs.
- We formulate the optimization problem to maximize the sum rate of users in the group sharing the same RB by optimizing the common data rate and beamformers of common and private messages. The resulting problem is non-convex, and we develop an efficient iterative algorithm based on the successive convex approximation (SCA) framework [17] to solve this problem in an iterative fashion, which arrives at least a local optimum.
- To model the RB adaptation of the users, we adopt the traditional evolutionary game (TEG) by leveraging the replicator dynamic process. This approach allows switching among RBs to achieve higher data rate. We then prove that the TEG approach is able to converge to an equilibrium at which the users do not have an incentive to switch their RB selection.
- To capture the impact of the users' memory on their decision-making, we reformulate TEG to FEG by accounting for the users' memory effect since users are actually aware of their historical experience before decision-making. We theoretically analyze and prove the unique equilibrium of the FEG approach.
- Extensive numerical results are provided to validate the theoretical analysis of the proposed approaches as well as to confirm their effectiveness. Specifically, we provide results related to the direction field of the replicator dynamics to validate the stability of the equilibrium. The numerical results also reveal that both the TEG and FEG approaches still reach their equilibrium under outdated information. Interestingly, the FEG outperforms TEG by exploiting the outdated information more effectively for decision-making.

The rest of the paper is organized as follows. In Section III, we present the system model and formulate an optimization problem in a general case. In Section IV, we develop a SCA algorithm to solve the sum rate optimization problem for the general case. In Section V, we present the expected data rate and utility of users. In Section VI, we formulate the dynamic RB selection problem by using the TEG and FEG approaches. Simulation results and discussions are provided Section VII, while Section VIII concludes the paper.

Notation: Throughout the paper, vectors and scalars are denoted by bold lowercase and lowercase letters. $\mathbb{C}$ represents the space of complex matrices and vectors. $(\cdot)^*$ and $(\cdot)^H$ denote the conjugate of a complex number and the conjugate transpose of a matrix or vector, respectively. $\mathcal{CN}(\mu, \sigma^2)$ represents circularly symmetric complex Gaussian distribution with mean μ and variance σ^2.

II. Related Works

A. Rate Splitting Multiple Access (RSMA) Approaches

Recently, several works related to RSMA have been investigated, and a comprehensive survey on RSMA can be found in [2]. Considering an RSMA-enabled single input single output (SISO) system, the work in [18] aimed to maximize the sum rate by jointly optimizing the common rate, transmit power of the common message, and transmit power of the private messages under successful SIC power requirements. The simulation results show that by simultaneously transmitting signals to all users at the same frequency, the RSMA scheme outperforms the SDMA scheme in terms of sum rate. However, this work considers the scenario with a single-antenna BS, which can limit the data rate achieved by the users. For this, RSMA-enabled multi-user multiple input single output (MISO) systems, e.g., [19] and [20], are considered. In such a work, the optimal common rate allocation and beamformer design are jointly considered. In particular, the work in [19] studied the problem of maximizing the total rate of users by optimizing the beamformers associated with the common and private messages given the imperfect channel state information (CSI). This work shows that compared with the no-RSMA scheme, the RSMA scheme is able to boost the achievable Degrees of Freedom (DoF) given certain CSI error. The simulation results show that the RSMA scheme outperforms the no-RSMA scheme in terms of ergodic sum rate, especially SNR $\geq$15 dB. Apart from the sum rate, the existing work related to RSMA aims to maximize the minimum rate among all users, *i.e.* max-min fairness, as presented in [21]. Then, the authors in [21] proposed a robust algorithm based on the cutting-set method coupled with the Weighted Minimum Mean Square Error (WMMSE) to solve the max-min fairness problem. The same problem is found in [22]. However, the work in [22] investigated the fairness problem under two CSI scenarios, *i.e.* the transmitter knows the Rayleigh fading channels with spatial correlations, and the transmitter knows the uniform linear array deployment with channel amplitudes and mean of phase. The numerical results show that the RSMA scheme

significantly gains the max-min fairness over the SDMA scheme in both scenarios. To enhance the data rate of the users, multiple subcarriers are considered in RSMA as presented in [23]. In this work, the users are divided into groups, and the users in a group share the same subcarrier. Then, the RSMA is applied to the group. The work aims to optimize the subcarrier allocation and beamformers in each group to maximize the total max-min fairness over groups. Recently, RSMA has been combined with enabling technologies in beyond 5G networks. In particular, RSMA is shown to efficiently manage the inter-beam interference for satellite communications [24]. Its application for simultaneous wireless information and power transfer (SWIPT) was also investigated in [25] to improve the sum rate of information receivers (IRs) compared with NOMA-based SWIPT. Combination of RSMA and intelligent reflecting surface (IRS) was studied in [26], aiming to improve the energy efficiency and reduce the outage probability [27]. The beamformer associated with the common message in RSMA can effectively manage interference. Thus, RSMA is integrated with a radar system, namely RSMA-based dual-function radar communication (DFRC), as proposed in [28] and [29], that is shown to improve the communication performance and radar performance as well as reduce the hardware size and cost.

B. Evolutionary Game Approaches

As mentioned earlier, the equilibrium of the evolutionary game, if existing, is important in the area of communication and networking since it guarantees the long-term stability of the network. Evolutionary game has been widely adopted to model the dynamic network selection of mobile users. In particular, the authors in [13] investigated the evolutionary game for the dynamic access network selection of the users in heterogeneous wireless access networks, i.e., WiFi and cellular networks. The utility of each user is a function of the achievable network capacity and the network cost. Similarly, the authors in [30] considered the access mode selection in a multitier cellular network, i.e., sub-6 GHz/mmWave cellular networks. Therein, the strategy of each mobile user is to select a tier to maximize its utility, which is a function of SINR and handover cost. Evolutionary game is adopted to model the dynamic tier selection of each user. The same problem can be found in [31], but the utility of each user is a function of achievable data rate and service cost. Apart from the network tier selection, evolutionary game is used to model the dynamic network resource/service selection of mobile users. In particular, the authors in [14] proposed to use the evolutionary game for the dynamic selection on communication services, i.e., including active data transmission or data backscatter. Considering an IRS-assisted network, the authors in [15] and [16] adopted the evolutionary game to model the dynamic selection on NRs, i.e., IRS modules and power level of the users. Both the theoretical analysis and simulation results in [15] and [16] showed that the evolutionary game approach assures a unique Nash equilibrium. The authors in [32] leveraged the evolutionary game to model the channel selection of self-interest-driven vehicular nodes. The utility of each vehicular node is expressed by the average number of packets that the node successfully transmits. The evolutionary game can be used to model the dynamic network service providers. Specifically, the authors in [33] considered a spectrum secondary market of cognitive radio networks. In the market, secondary providers provide spectrum resources to secondary users. Different secondary providers can set different prices for their spectrum resources. Therefore, the secondary users select a service provider based on its perceived instantaneous utility, which depends on the allocated spectrum and spectrum cost. The evolutionary game is used to address the dynamic service provider selection of the secondary users. The authors in [34] considered an UAV-assisted Metaverse system in which UAVs as IoT devices collect sensing data for digital twin synchronization of virtual service providers (VSPs). Each UAV receives an incentive reward for its data collection. Different VSPs have different incentive pools, and thus each UAV needs to make its VSP selection to achieve the highest incentive reward. Evolutionary game is then used to model the dynamic VSP selection of the UAVs.

Different from the aforementioned works, the work in [35] investigated the access mode selection problem of D2D users in fog radio access networks. The strategy of each D2D user is to select the access mode, i.e., a nearby D2D user or a fog node, for its content request. Its utility is a function of ergodic rate and delay cost. Then, the competition among the groups of the D2D users is formulated as a dynamic evolutionary game. The aforementioned evolutionary game approaches are summarized in Table I, while a comprehensive survey of RSMA approaches can be referred to [2].

III. System Model and Problem Formulation

In this section, we first present the RSMA-enabled network with multiple RBs, and then formulate the problem formulation for a general case where users select the same RB. Each RB is an NR, and thus in the rest of the paper, "RB" and "NR" can be used interchangeably.

A. Network Model

We consider a downlink RSMA system that consists of a BS serving a set $\mathcal{N}$ of N users as shown in Fig. 1. The BS is equipped with L antennas and has a set $\mathcal{K}$ of K NRs. The bandwidth of each NR is determined according to the 5G standard [36]. In particular, each NR $k \in \mathcal{K}$ has 12 subcarriers and the frequency spacing of each subcarrier is 15 kHz. Therefore, the bandwidth of NR k is $B_k = 12 \times 15 \times 2^{\alpha}$ kHz, where $\alpha \in \{0, 1, 2, 3, 4\}$ is the numerology. Each user only occupies at most one NR in one time slot, but the NR can be occupied by multiple users for the rate-splitting purpose. In future networks, users are able to dynamically decide the NR that yields to higher data rate and utility depending on their channel conditions. Thus, in this work we consider a dynamic and decentralized network in which each user can dynamically select an NR over time. Assuming that there is a set $\mathcal{N}_k$ of $N_k \geq 0$ users selecting NR k. As $N_k = 0$, no user selects NR k. The BS then adopts RSMA for users selecting the same NR. With RSMA, the BS transmits i) a common message

TABLE I
SUMMARY OF EVOLUTIONARY GAME APPROACHES FOR COMMUNICATION AND NETWORKING

Refs.	Scenario	Player	Strategy	Utility/payoff
[13]	HetNet	Mobile users	Access network selection	Network capacity and service cost
[14]	Backscatter-assisted cognitive radio network	Secondary transmitter	Access point, active transmission, and backscatter selection	Amount of transmitted data and service cost
[15] and [16]	IRS-assisted cellular network	Mobile user	Base station, IRS module, and power level selection	Data rate and service cost
[29]	Multi-tier cellular network	Mobile user	Network tier selection	SINR and handover cost
[30]	Multi-tier cellular network	Mobile user	Network tier selection	Data rate and service cost
[31]	Cognitive vehicular networks	Vehicular node	Channel selection	Average number of successfully-transmitted packets
[32]	Cognitive radio network	Secondary user	Spectrum provider selection	Allocated spectrum and spectrum cost
[33]	UAV-assisted Metaverse system	UAVs	Virtual service provider selection	Incentive cost
[34]	Fog radio access network	D2D user	Nearby D2D user and fog node selection	Ergodic rate and delay cost

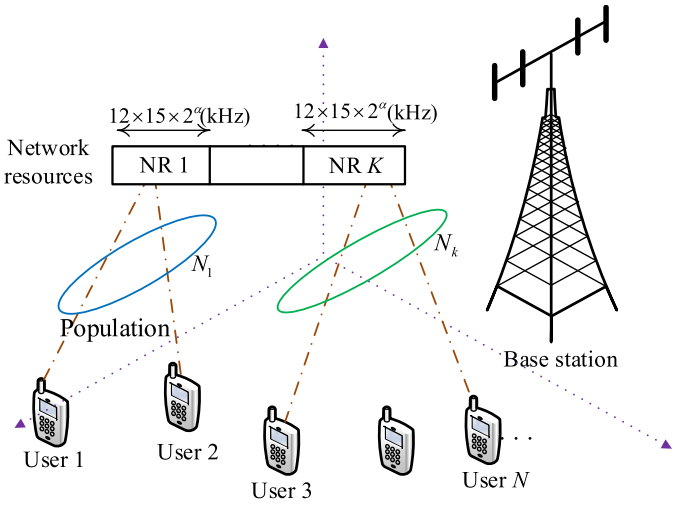

Fig. 1. Dynamic network resource selection in an RSMA system.

to all users in the group and *ii*) the private massages to the intended users in the group. For convenience, we name the transmit power of the common message as *common power* and the transmit power of the private messages as *private power*. Before transmitting the messages to each group, the BS needs to optimize beamformers associated with the common and private messages, which will be presented in the next section.

B. Rate-Splitting Multiple Access Scheme

Without loss of generality, we focus on group k and assume that user $i \in \mathcal{N}$ selects NR k. We define $\mathbf{s}_k \triangleq [s_{k,0}, s_{k,1}, \ldots, s_{k,N_k}]$ where $s_{k,0}$ is the common message transmitted by the BS to group k, $s_{k,i}$ is the private message transmitted by the BS to user i in group k, and $\mathbb{E}\left[\mathbf{s}_k^H \mathbf{s}_k\right] = \mathbf{I}$. We further denote $\mathbf{w}_{k,0} \in \mathbb{C}^{L\times 1}$ as the beamformer associated with the common message, and $\mathbf{w}_{k,i} \in \mathbb{C}^{L\times 1}$ as the beamformer associated with the private message of user i in group k. By $\mathbf{w}_k \triangleq [\mathbf{w}_{k,0}, \mathbf{w}_{k,1}, \ldots, \mathbf{w}_{k,N_k}]$, the per-group power constraint can be expressed as [37]:

$$\mathrm{tr}\left(\mathbf{w}_k \mathbf{w}_k^H\right) \leq P_k \tag{1}$$

where P_k is the power budget allocated (by the BS) to NR k. To guarantee the fairness among groups, P_k is determined as $P_k = P_{\max}/K$, where $P_{\max}$ is the power budget of the BS. The signal intended to group k transmitted by the BS is given by

$$\mathbf{x}_k = \mathbf{w}_{k,0} s_{k,0} + \sum_{j\in\mathcal{N}_k} \mathbf{w}_{k,j} s_{k,j}. \tag{2}$$

Accordingly, the received signal at user i selecting NR k is [26]

$$y_{k,i} = \mathbf{h}_{k,i}^H \left(\mathbf{w}_{k,0} s_{k,0} + \sum_{j\in\mathcal{N}_k} \mathbf{w}_{k,j} s_{k,j}\right) + \omega_{k,i} \tag{3}$$

where $\mathbf{h}_{k,i} \in \mathbb{C}^{L\times 1}$ is the channel from the BS to user i and $\omega_{k,i}$ is the additive noise with variance σ_0^2.

The data rate achieved by user i for decoding the common message is given by

$$R_{k,i}^0 = B_k \log_2\left(1 + \frac{|\mathbf{h}_{k,i}^H \mathbf{w}_{k,0}|^2}{\sum_{j\in\mathcal{N}_k} |\mathbf{h}_{k,i}^H \mathbf{w}_{k,j}|^2 + B_k \sigma^2}\right). \tag{4}$$

To guarantee that all users in a group (say group k) can successfully decode the common message with RSMA, the BS needs to transmit the common message at a rate of

$$R_k^0 = \min_{i\in\mathcal{N}_k} \left\{R_{k,i}^0\right\}. \tag{5}$$

Let $C_{k,i}^0$ be the allocated common data rate of user i in group k. The following rate constraint is imposed [26]

$$\sum_{i\in\mathcal{N}_k} C_{k,i}^0 \leq R_k^0. \tag{6}$$

The common message is then removed by SIC before decoding the private message. The achievable rate of the private message of user i in group k is given by

$$R_{k,i} = B_k \log_2\left(1 + \frac{|\mathbf{h}_{k,i}^H \mathbf{w}_{k,i}|^2}{\sum_{j\in\mathcal{N}_k, j\neq i} |\mathbf{h}_{k,i}^H \mathbf{w}_{k,j}|^2 + B_k \sigma^2}\right). \tag{7}$$

The total transmission rate of user i in group k is the sum of its common message rate $C_{k,i}^0$ and private message rate $R_{k,i}$, given as

$$R_{k,i}^{\mathrm{tot}} = C_{k,i}^0 + R_{k,i}. \tag{8}$$

C. Problem Formulation

For every group adopted RSMA, we aim to maximize the sum rate of all users in the same group by optimizing i) the common data rate, ii) beamformer associated with the common message, and iii) beamformers associated with the private messages. The optimization problem for group k is mathematically formulated as follows

$$\max_{\mathbf{w}_{k,0},\left\{C^0_{k,i},\mathbf{w}_{k,i}\right\}_{i\in\mathcal{N}_k}} f(C^0_{k,i},\mathbf{w}_{k,i}) \triangleq \sum_{i\in\mathcal{N}_k}\left(C^0_{k,i}+R_{k,i}\right) \tag{9a}$$

$$\text{s.t.} \sum_{i\in\mathcal{N}_k} C^0_{k,i} \le R^0_k \tag{9b}$$

$$\text{tr}\left(\mathbf{w}_k\mathbf{w}_k^H\right) \le P_k. \tag{9c}$$

The optimization problem given in (9) is non-convex due to the non-concavity of the objective function (9a) and non-convexity of constraint (9b), which results in difficulty for obtaining a global optimal solution. In the next section, we will leverage the SCA framework [17] to convexify the optimization problem (9) and thereafter develop an iterative algorithm to obtain its solution.

IV. Successive Convex Approximation Algorithm

Let $\left(\mathbf{w}^{\langle\kappa\rangle}_{k,0},\left\{C^{0,\langle\kappa\rangle}_{k,i},\mathbf{w}^{\langle\kappa\rangle}_{k,i}\right\}_{i\in\mathcal{N}_k}\right)$ be a feasible point for (9) found from the $\langle\kappa-1\rangle$-th iteration. In iteration κ, we determine the next feasible point $\left(\mathbf{w}^{\langle\kappa+1\rangle}_{k,0},\left\{C^{0\langle\kappa+1\rangle}_{k,i},\mathbf{w}^{\langle\kappa+1\rangle}_{k,i}\right\}_{i\in\mathcal{N}_k}\right)$. Considering user $i\in\mathcal{N}_k$ in the objective function, we first apply the inequality (A.3) in Appendix A to the private data rate of $R_{k,i}$ with $x = \left|\mathbf{h}^H_{k,i}\mathbf{w}_{k,i}\right|^2$, $y = \sum_{j\in\mathcal{N}_k,j\neq i}\left|\mathbf{h}^H_{k,i}\mathbf{w}_{k,j}\right|^2 + B_k\sigma^2$, and $\bar{x} = \left|\mathbf{h}^H_{k,i}\mathbf{w}^{\langle\kappa\rangle}_{k,i}\right|^2, \bar{y} = \sum_{j\in\mathcal{N}_k,j\neq i}\left|\mathbf{h}^H_{k,i}\mathbf{w}^{\langle\kappa\rangle}_{k,j}\right|^2 + B_k\sigma^2$. Then, by using the first-order Taylor approximation, $R_{k,i}$ can be approximated by the concave function $R^{\langle\kappa\rangle}_{k,i}$ given in (11), as shown at the bottom of the next page, over the trust region defined by

$$2\Re\left\{\left(\mathbf{h}^H_{k,i}\mathbf{w}_{k,i}\right)\left(\mathbf{h}^H_{k,i}\mathbf{w}^{\langle\kappa\rangle}_{k,i}\right)^*\right\} - \left|\mathbf{h}^H_{k,i}\mathbf{w}^{\langle\kappa\rangle}_{k,i}\right|^2 \ge 0,\ \forall i \tag{10}$$

with

$$0 < a^{\langle\kappa\rangle}_{k,i} = B_k\log_2\left(1+\frac{\left|\mathbf{h}^H_{k,i}\mathbf{w}^{\langle\kappa\rangle}_{k,i}\right|^2}{\sum_{j\in\mathcal{N}_k,j\neq i}\left|\mathbf{h}^H_{k,i}\mathbf{w}^{\langle\kappa\rangle}_{k,j}\right|^2+B_k\sigma^2}\right)$$

and

$$0 < b^{\langle\kappa\rangle}_{k,i} = \frac{\frac{B_k\left|\mathbf{h}^H_{k,i}\mathbf{w}^{\langle\kappa\rangle}_{k,i}\right|^2}{\sum_{j\in\mathcal{N}_k,j\neq i}\left|\mathbf{h}^H_{k,i}\mathbf{w}^{\langle\kappa\rangle}_{k,j}\right|^2+B_k\sigma^2}}{\ln 2\left(1+\frac{\left|\mathbf{h}^H_{k,i}\mathbf{w}^{\langle\kappa\rangle}_{k,i}\right|^2}{\sum_{j\in\mathcal{N}_k,j\neq i}\left|\mathbf{h}^H_{k,i}\mathbf{w}^{\langle\kappa\rangle}_{k,j}\right|^2+B_k\sigma^2}\right)}.$$

From (11), we can approximate the objective function in (9) by the following concave function

$$\begin{aligned} f(C^0_{k,i},\mathbf{w}_{k,i}) &\ge \sum_{i\in\mathcal{N}_k}\left(C^0_{k,i}+R^{\langle\kappa\rangle}_{k,i}\right) \\ &= f^{\langle\kappa\rangle}(C^0_{k,i},\mathbf{w}_{k,i}). \end{aligned} \tag{12}$$

Next, we tackle constraint (9b). Similarly, we apply the inequality given in (A.3) to $R^0_{k,i}$ with $x = \left|\mathbf{h}^H_{k,i}\mathbf{w}_{k,0}\right|^2$, $\bar{x} = \left|\mathbf{h}^H_{k,i}\mathbf{w}^{\langle\kappa\rangle}_{k,0}\right|^2, y = \sum_{j\in\mathcal{N}_k}\left|\mathbf{h}^H_{k,i}\mathbf{w}_{k,j}\right|^2 + B_k\sigma^2, \bar{y} = \sum_{j\in\mathcal{N}_k}\left|\mathbf{h}^H_{k,i}\mathbf{w}^{\langle\kappa\rangle}_{k,j}\right|^2 + B_k\sigma^2$. Then, by using the first-order Taylor approximation, $R^0_{k,i}$ is approximated by the concave function $R^{0\ \langle\kappa\rangle}_{k,i}$ given in (13), as shown at the bottom of the next page, over the trust region defined by

$$2\Re\left\{\left(\mathbf{h}^H_{k,i}\mathbf{w}_{k,0}\right)\left(\mathbf{h}^H_{k,i}\mathbf{w}^{\langle\kappa\rangle}_{k,0}\right)^*\right\} - \left|\mathbf{h}^H_{k,i}\mathbf{w}^{\langle\kappa\rangle}_{k,0}\right|^2 \ge 0 \tag{14}$$

with

$$0 < a^{0,\langle\kappa\rangle}_{k,i} = B_k\log_2\left(1+\frac{\left|\mathbf{h}^H_{k,i}\mathbf{w}^{\langle\kappa\rangle}_{k,0}\right|^2}{\sum_{j\in\mathcal{N}_k}\left|\mathbf{h}^H_{k,i}\mathbf{w}^{\langle\kappa\rangle}_{k,j}\right|^2+B_k\sigma^2}\right)$$

and

$$0 < b^{0,\langle\kappa\rangle}_{k,i} = \frac{\frac{B_k\left|\mathbf{h}^H_{k,i}\mathbf{w}^{\langle\kappa\rangle}_{k,0}\right|^2}{\sum_{j\in\mathcal{N}_k}\left|\mathbf{h}^H_{k,i}\mathbf{w}^{\langle\kappa\rangle}_{k,j}\right|^2+B_k\sigma^2}}{\ln 2\left(1+\frac{\left|\mathbf{h}^H_{k,i}\mathbf{w}^{\langle\kappa\rangle}_{k,0}\right|^2}{\sum_{j\in\mathcal{N}_k}\left|\mathbf{h}^H_{k,i}\mathbf{w}^{\langle\kappa\rangle}_{k,j}\right|^2+B_k\sigma^2}\right)}.$$

Using (13), the nonconvex constraint in (9b) can be interactively replaced by the following convex constraint

$$\sum_{i\in\mathcal{N}_k} C^0_{k,i} \le R^{0,\langle\kappa\rangle}_k = \min_{i\in\mathcal{N}_k}\left\{R^{0,\langle\kappa\rangle}_{k,i}\right\}. \tag{15}$$

From the above developments, the approximate convex program of (9) solved at iteration κ is given as

$$\max_{\mathbf{w}_{k,0},\left\{C^0_{k,i},\mathbf{w}_{k,i}\right\}_{i\in\mathcal{N}_k}} f^{\langle\kappa\rangle}(C^0_{k,i},\mathbf{w}_{k,i}) \tag{16a}$$

$$\text{s.t. } (9c),(10),(14),(15). \tag{16b}$$

A. Generating an Initial Feasible Point

We note that the approximate convex problem (16) requires an initial feasible point to start the iterative algorithm successfully at the first iterations. In doing so, we first take any value for $C^{0,\langle 0\rangle}_{k,i}$ and randomly generate an initial point $\left(\mathbf{w}^{\langle 0\rangle}_{k,0},\left\{\mathbf{w}^{\langle 0\rangle}_{k,i}\right\}_{i\in\mathcal{N}_k}\right)$ for (9c). Then, we solve the following simplified problem of (16):

$$\max_{\mathbf{w}_{k,0},\left\{\mathbf{w}_{k,i}\right\}_{i\in\mathcal{N}_k}} R^{0,\langle\kappa\rangle}_k - \sum_{i\in\mathcal{N}_k} C^{0,\langle 0\rangle}_{k,i} \tag{17a}$$

$$\text{s.t. } (9c),(10),(14) \tag{17b}$$

until reaching a positive objective value, such as $R^{0,\langle\kappa\rangle}_k - \sum_{i\in\mathcal{N}_k} C^{0,\langle 0\rangle}_{k,i} \ge 0$. Solving (17) generates a feasible set of $\left(\mathbf{w}^{\langle\kappa\rangle}_{k,0},\left\{C^{0,\langle 0\rangle}_{k,i},\mathbf{w}^{\langle\kappa\rangle}_{k,i}\right\}_{i\in\mathcal{N}_k}\right)$ that is considered to be an initial feasible point for (16). The proposed SCA-based iterative algorithm for solving the non-convex problem in (9) is summarized in Algorithm 1.

B. Convergence and Complexity Analysis

We now discuss the convergence of the proposed SCA-based Algorithm 1. Since $\left(\mathbf{w}^{\langle\kappa\rangle}_{k,0},\left\{C^{0,\langle\kappa\rangle}_{k,i},\mathbf{w}^{\langle\kappa\rangle}_{k,i}\right\}_{i\in\mathcal{N}_k}\right)$ and $\left(\mathbf{w}^{\langle\kappa+1\rangle}_{k,0},\left\{C^{0,\langle\kappa+1\rangle}_{k,i},\mathbf{w}^{\langle\kappa+1\rangle}_{k,i}\right\}_{i\in\mathcal{N}_k}\right)$ are the feasible point and the optimal solution to (16), respectively, we can show that

$$f^{\langle\kappa\rangle}\left(\mathbf{w}^{\langle\kappa+1\rangle}_{k,0},\mathbf{w}^{\langle\kappa+1\rangle}_{k,i}\right) > f^{\langle\kappa\rangle}\left(\mathbf{w}^{\langle\kappa\rangle}_{k,0},\mathbf{w}^{\langle\kappa\rangle}_{k,i}\right),\ \forall i\in\mathcal{N}_k \tag{18}$$

Algorithm 1 Iterative Algorithm for Problem (9)

Initialization: Take any value of $C_{k,i}^{0,\langle 0\rangle}$, generate an initial point $\left(\mathbf{w}_{k,0}^{\langle 0\rangle}, \left\{\mathbf{w}_{k,i}^{\langle 0\rangle}\right\}_{i\in\mathcal{N}_k}\right)$ for (9c), and iterate (17) for a feasible point $\left(\mathbf{w}_{k,0}^{\langle \kappa\rangle}, \left\{C_{k,i}^{0,\langle 0\rangle}, \mathbf{w}_{k,i}^{\langle \kappa\rangle}\right\}_{i\in\mathcal{N}_k}\right)$ for (16). Set $\kappa = 0$.

1: **repeat**
2: Solve the convex program (16) to obtain the optimal solution $\left(\mathbf{w}_{k,0}^{\star}, \left\{C_{k,i}^{0,\star}, \mathbf{w}_{k,i}^{\star}\right\}_{i\in\mathcal{N}_k}\right)$
3: Update $\left(\mathbf{w}_{k,0}^{\langle \kappa+1\rangle}, \left\{C_{k,i}^{0,\langle \kappa+1\rangle}, \mathbf{w}_{k,i}^{\langle \kappa+1\rangle}\right\}_{i\in\mathcal{N}_k}\right) := \left(\mathbf{w}_{k,0}^{\star}, \left\{C_{k,i}^{0,\star}, \mathbf{w}_{k,i}^{\star}\right\}_{i\in\mathcal{N}_k}\right)$
4: Set $\kappa \leftarrow \kappa + 1$
5: **until** Convergence

for any $\left(\mathbf{w}_{k,0}^{\langle \kappa\rangle}, \left\{C_{k,i}^{0,\langle \kappa\rangle}, \mathbf{w}_{k,i}^{\langle \kappa\rangle}\right\}_{i\in\mathcal{N}_k}\right) \neq \left(\mathbf{w}_{k,0}^{\langle \kappa+1\rangle}, \left\{C_{k,i}^{0,\langle \kappa+1\rangle}, \mathbf{w}_{k,i}^{\langle \kappa+1\rangle}\right\}_{i\in\mathcal{N}_k}\right)$. It simply means that $\left(\mathbf{w}_{k,0}^{\langle \kappa+1\rangle}, \left\{C_{k,i}^{0,\langle \kappa+1\rangle}, \mathbf{w}_{k,i}^{\langle \kappa+1\rangle}\right\}_{i\in\mathcal{N}_k}\right)$ is a better point to (16) than $\left(\mathbf{w}_{k,0}^{\langle \kappa\rangle}, \left\{C_{k,i}^{0,\langle \kappa\rangle}, \mathbf{w}_{k,i}^{\langle \kappa\rangle}\right\}_{i\in\mathcal{N}_k}\right)$. Considering (12), it is true that [38] and [39]:

$$f\left(\mathbf{w}_{k,0}^{\langle \kappa\rangle}, \mathbf{w}_{k,i}^{\langle \kappa\rangle}\right) = f^{\langle \kappa\rangle}\left(\mathbf{w}_{k,0}^{\langle \kappa\rangle}, \mathbf{w}_{k,i}^{\langle \kappa\rangle}\right) \tag{19}$$

$$< f^{\langle \kappa\rangle}\left(\mathbf{w}_{k,0}^{\langle \kappa+1\rangle}, \mathbf{w}_{k,i}^{\langle \kappa+1\rangle}\right) \tag{20}$$

$$\leq f\left(\mathbf{w}_{k,0}^{\langle \kappa+1\rangle}, \mathbf{w}_{k,i}^{\langle \kappa+1\rangle}\right). \tag{21}$$

This clearly shows that the optimal solution $\left(\mathbf{w}_{k,0}^{\langle \kappa+1\rangle}, \left\{C_{k,i}^{0,\langle \kappa+1\rangle}, \mathbf{w}_{k,i}^{\langle \kappa+1\rangle}\right\}_{i\in\mathcal{N}_k}\right)$ of (16) satisfies the convergence condition: $f\left(\mathbf{w}_{k,0}^{\langle \kappa+1\rangle}, \mathbf{w}_{k,i}^{\langle \kappa+1\rangle}\right) > f\left(\mathbf{w}_{k,0}^{\langle \kappa\rangle}, \mathbf{w}_{k,i}^{\langle \kappa\rangle}\right), \forall i \in \mathcal{N}_k$. The sequence $\left(\mathbf{w}_{k,0}^{\langle \kappa+1\rangle}, \mathbf{w}_{k,i}^{\langle \kappa+1\rangle}\right)$ converges to a saddle point $\left(\bar{\mathbf{w}}_{k,0}, \bar{\mathbf{w}}_{k,i}\right)$ after a sufficiently large number of iterations [39]. The numbers of decision variables and convex constraints in solving (16) are $L + N_k + LN_k$ and $2N_k + 2$, respectively. Thus, the worst-case computational complexity per iteration of Algorithm 1 is $\mathcal{O}\left(\sqrt{2N_k}(L + N_k + LN_k)^3\right)$ [40].

V. Expected Data Rate and Utility

The data rate achieved by each user depends on the number of remaining users selecting the same NR due to interference. Meanwhile, the NR selection of each user is random, and thus we need to determine the expected data rate that all users can obtain. We let $x_{k,i}$ be the probability that user $i \in \mathcal{N}$ selects NR $k \in \mathcal{K}$. To simply present the data rate achieved by user i, we consider the case with three users, *i.e.* $N = 3$. A general scenario with more than 3 users can be investigated in the same way. We denote $x_{k,1}$, $x_{k,2}$, and $x_{k,3}$ as the probabilities that users 1, 2 and 3 select NR k, respectively. In this example, the expected data rate of users can be presented as follows.

A. Expected Data Rate

There are seven possible cases for the user association as follows.

1) Case 1 - All Users Select NR k: In this case, all users belong to group k (*i.e.* $\mathcal{N}_k = \{1, 2, 3\}$) with the probability of $x_{k,1}x_{k,2}x_{k,3}$. Therein, user 1 suffers interference from both users 2 and 3, and vice versa. The data rates obtained by users 1, 2 and 3 are given by

$$R_{k,1}^{\text{tot},\{1,2,3\}} = C_{k,1}^{0,\{1,2,3\}} + B_k \log_2\left(1 + \frac{\left|\mathbf{h}_{k,1}^H \mathbf{w}_{k,1}^{\{1,2,3\}}\right|^2}{\left|\mathbf{h}_{k,1}^H \mathbf{w}_{k,2}^{\{1,2,3\}}\right|^2 + \left|\mathbf{h}_{k,1}^H \mathbf{w}_{k,3}^{\{1,2,3\}}\right|^2 + B_k\sigma^2}\right), \tag{22}$$

$$R_{k,2}^{\text{tot},\{1,2,3\}} = C_{k,2}^{0,\{1,2,3\}} + B_k \log_2\left(1 + \frac{\left|\mathbf{h}_{k,2}^H \mathbf{w}_{k,2}^{\{1,2,3\}}\right|^2}{\left|\mathbf{h}_{k,2}^H \mathbf{w}_{k,1}^{\{1,2,3\}}\right|^2 + \left|\mathbf{h}_{k,2}^H \mathbf{w}_{k,3}^{\{1,2,3\}}\right|^2 + B_k\sigma^2}\right) \tag{23}$$

$$\begin{aligned} R_{k,i} &\geq a_{k,i}^{\langle \kappa\rangle} + b_{k,i}^{\langle \kappa\rangle}\left(2 - \frac{\left|\mathbf{h}_{k,i}^H \mathbf{w}_{k,i}^{\langle \kappa\rangle}\right|^2}{\left|\mathbf{h}_{k,i}^H \mathbf{w}_{k,i}\right|^2} - \frac{\sum_{j\in\mathcal{N}_k, j\neq i}\left|\mathbf{h}_{k,i}^H \mathbf{w}_{k,j}\right|^2 + B_k\sigma^2}{\sum_{j\in\mathcal{N}_k, j\neq i}\left|\mathbf{h}_{k,i}^H \mathbf{w}_{k,j}^{\langle \kappa\rangle}\right|^2 + B_k\sigma^2}\right) \\ &\geq a_{k,i}^{\langle \kappa\rangle} + b_{k,i}^{\langle \kappa\rangle}\left(2 - \frac{\left|\mathbf{h}_{k,i}^H \mathbf{w}_{k,i}^{\langle \kappa\rangle}\right|^2}{2\Re\left\{\left(\mathbf{h}_{k,i}^H \mathbf{w}_{k,i}\right)\left(\mathbf{h}_{k,i}^H \mathbf{w}_{k,i}^{\langle \kappa\rangle}\right)^*\right\} - \left|\mathbf{h}_{k,i}^H \mathbf{w}_{k,i}^{\langle \kappa\rangle}\right|^2} - \frac{\sum_{j\in\mathcal{N}_k, j\neq i}\left|\mathbf{h}_{k,i}^H \mathbf{w}_{k,j}\right|^2 + B_k\sigma^2}{\sum_{j\in\mathcal{N}_k, j\neq i}\left|\mathbf{h}_{k,i}^H \mathbf{w}_{k,j}^{\langle \kappa\rangle}\right|^2 + B_k\sigma^2}\right) \\ &\triangleq R_{k,i}^{\langle \kappa\rangle}. \end{aligned} \tag{11}$$

$$\begin{aligned} R_{k,i}^0 &\geq a_{k,i}^{0,\langle \kappa\rangle} + b_{k,i}^{0,\langle \kappa\rangle}\left(2 - \frac{\left|\mathbf{h}_{k,i}^H \mathbf{w}_{k,0}^{\langle \kappa\rangle}\right|^2}{\left|\mathbf{h}_{k,i}^H \mathbf{w}_{k,0}\right|^2} - \frac{\sum_{j\in\mathcal{N}_k}\left|\mathbf{h}_{k,i}^H \mathbf{w}_{k,j}\right|^2 + B_k\sigma^2}{\sum_{j\in\mathcal{N}_k}\left|\mathbf{h}_{k,i}^H \mathbf{w}_{k,j}^{\langle \kappa\rangle}\right|^2 + B_k\sigma^2}\right) \\ &\geq a_{k,i}^{0,\langle \kappa\rangle} + b_{k,i}^{0,\langle \kappa\rangle}\left(2 - \frac{\left|\mathbf{h}_{k,i}^H \mathbf{w}_{k,0}^{\langle \kappa\rangle}\right|^2}{2\Re\left\{\left(\mathbf{h}_{k,i}^H \mathbf{w}_{k,0}\right)\left(\mathbf{h}_{k,i}^H \mathbf{w}_{k,0}^{\langle \kappa\rangle}\right)^*\right\} - \left|\mathbf{h}_{k,i}^H \mathbf{w}_{k,0}^{\langle \kappa\rangle}\right|^2} - \frac{\sum_{j\in\mathcal{N}_k}\left|\mathbf{h}_{k,i}^H \mathbf{w}_{k,j}\right|^2 + B_k\sigma^2}{\sum_{j\in\mathcal{N}_k}\left|\mathbf{h}_{k,i}^H \mathbf{w}_{k,j}^{\langle \kappa\rangle}\right|^2 + B_k\sigma^2}\right) \\ &\triangleq R_{k,i}^{0\ \langle \kappa\rangle}. \end{aligned} \tag{13}$$

and

$$R_{k,3}^{\mathrm{tot},\{1,2,3\}} = C_{k,3}^{0,\{1,2,3\}} + B_k \log_2\left(1+\frac{\left|\mathbf{h}_{k,3}^H \mathbf{w}_{k,3}^{\{1,2,3\}}\right|^2}{\left|\mathbf{h}_{k,3}^H \mathbf{w}_{k,1}^{\{1,2,3\}}\right|^2+\left|\mathbf{h}_{k,3}^H \mathbf{w}_{k,3}^{\{1,2,3\}}\right|^2 + B_k\sigma^2}\right), \tag{24}$$

respectively, where

$$C_{k,1}^{0,\{1,2,3\}} + C_{k,2}^{0,\{1,2,3\}} + C_{k,3}^{0,\{1,2,3\}} \leq \min\left\{R_{k,1}^{0,\{1,2,3\}}, R_{k,2}^{0,\{1,2,3\}}, R_{k,3}^{0,\{1,2,3\}}\right\} \tag{25}$$

with $R_{k,1}^{0,\{1,2,3\}}$, $R_{k,2}^{0,\{1,2,3\}}$, and $R_{k,3}^{0,\{1,2,3\}}$ being given in (26), as shown at the bottom of the next page.

2) Case 2 - Users 1 and 2 Select NR k While User 3 Does Not: In this case, users 1 and 2 belong to group k (*i.e.* $\mathcal{N}_k = \{1,2\}$) with the probability of $x_{k,1}x_{k,2}\left(1-x_{k,3}\right)$. Therein, user 1 suffers interference from user 2, and vice versa. The data rates obtained by users 1 and 2 are given by

$$R_{k,1}^{\mathrm{tot},\{1,2\}} = C_{k,1}^{0,\{1,2\}} + B_k \log_2\left(1+\frac{\left|\mathbf{h}_{k,1}^H \mathbf{w}_{k,1}^{\{1,2\}}\right|^2}{\left|\mathbf{h}_{k,1}^H \mathbf{w}_{k,2}^{\{1,2\}}\right|^2 + B_k\sigma^2}\right) \tag{27}$$

and

$$R_{k,2}^{\mathrm{tot},\{1,2\}} = C_{k,2}^{0,\{1,2\}} + B_k \log_2\left(1+\frac{\left|\mathbf{h}_{k,2}^H \mathbf{w}_{k,2}^{\{1,2\}}\right|^2}{\left|\mathbf{h}_{k,2}^H \mathbf{w}_{k,1}^{\{1,2\}}\right|^2 + B_k\sigma^2}\right) \tag{28}$$

respectively, where

$$C_{k,1}^{0,\{1,2\}} + C_{k,2}^{0,\{1,2\}} \leq \min\left\{R_{k,1}^{0,\{1,2\}}, R_{k,2}^{0,\{1,2\}}\right\} \tag{29}$$

with

$$R_{k,1}^{0,\{1,2\}} = B_k \log_2\left(1+\frac{\left|\mathbf{h}_{k,1}^H \mathbf{w}_{k,0}^{\{1,2\}}\right|^2}{\left|\mathbf{h}_{k,1}^H \mathbf{w}_{k,1}^{\{1,2\}}\right|^2 + \left|\mathbf{h}_{k,1}^H \mathbf{w}_{k,2}^{\{1,2\}}\right|^2 + B_k\sigma^2}\right) \tag{30}$$

$$R_{k,2}^{0,\{1,2\}} = B_k \log_2\left(1+\frac{\left|\mathbf{h}_{k,2}^H \mathbf{w}_{k,0}^{\{1,2\}}\right|^2}{\left|\mathbf{h}_{k,2}^H \mathbf{w}_{k,1}^{\{1,2\}}\right|^2 + \left|\mathbf{h}_{k,2}^H \mathbf{w}_{k,2}^{\{1,2\}}\right|^2 + B_k\sigma^2}\right). \tag{31}$$

3) Case 3 - Users 1 and 3 Select NR k While User 2 Does Not: In this case, users 1 and 3 belong to group k (*i.e.* $\mathcal{N}_k = \{1,3\}$) with the happening probability of $x_{k,1}\left(1-x_{k,2}\right)x_{k,3}$. Therein, user 1 suffers the interference from user 3, and vice versa. The data rates obtained by users 1 and 3 are given by

$$R_{k,1}^{\mathrm{tot},\{1,3\}} = C_{k,1}^{0,\{1,3\}} + B_k \log_2\left(1+\frac{\left|\mathbf{h}_{k,1}^H \mathbf{w}_{k,1}^{\{1,3\}}\right|^2}{\left|\mathbf{h}_{k,1}^H \mathbf{w}_{k,3}^{\{1,3\}}\right|^2 + B_k\sigma^2}\right) \tag{32}$$

and

$$R_{k,3}^{\mathrm{tot},\{1,3\}} = C_{k,3}^{0,\{1,3\}} + B_k \log_2\left(1+\frac{\left|\mathbf{h}_{k,3}^H \mathbf{w}_{k,3}^{\{1,3\}}\right|^2}{\left|\mathbf{h}_{k,3}^H \mathbf{w}_{k,1}^{\{1,3\}}\right|^2 + B_k\sigma^2}\right), \tag{33}$$

respectively, where

$$C_{k,1}^{0,\{1,3\}} + C_{k,3}^{0,\{1,3\}} \leq \min\left\{R_{k,1}^{0,\{1,3\}}, R_{k,3}^{0,\{1,3\}}\right\} \tag{34}$$

with

$$R_{k,1}^{0,\{1,3\}} = B_k \log_2\left(1+\frac{\left|\mathbf{h}_{k,1}^H \mathbf{w}_{k,0}^{\{1,3\}}\right|^2}{\left|\mathbf{h}_{k,1}^H \mathbf{w}_{k,1}^{\{1,3\}}\right|^2 + \left|\mathbf{h}_{k,1}^H \mathbf{w}_{k,3}^{\{1,3\}}\right|^2 + B_k\sigma^2}\right) \tag{35}$$

$$R_{k,3}^{0,\{1,3\}} = B_k \log_2\left(1+\frac{\left|\mathbf{h}_{k,3}^H \mathbf{w}_{k,0}^{\{1,3\}}\right|^2}{\left|\mathbf{h}_{k,3}^H \mathbf{w}_{k,1}^{\{1,3\}}\right|^2 + \left|\mathbf{h}_{k,3}^H \mathbf{w}_{k,3}^{\{1,3\}}\right|^2 + B_k\sigma^2}\right). \tag{36}$$

4) Case 4 - Users 2 and 3 Select NR k While User 1 Does Not: In this case, users 2 and 3 belong to group k (*i.e.* $\mathcal{N}_k = \{2,3\}$) with the happening probability of $\left(1-x_{k,1}\right)x_{k,2}x_{k,3}$. Therein, user 2 suffers the interference from user 3, and vice versa. The data rates obtained by users 2 and 3 are given by

$$R_{k,2}^{\mathrm{tot},\{2,3\}} = C_{k,2}^{0,\{2,3\}} + B_k \log_2\left(1+\frac{\left|\mathbf{h}_{k,2}^H \mathbf{w}_{k,2}^{\{2,3\}}\right|^2}{\left|\mathbf{h}_{k,2}^H \mathbf{w}_{k,3}^{\{2,3\}}\right|^2 + B_k\sigma^2}\right) \tag{37}$$

and

$$R_{k,3}^{\mathrm{tot},\{2,3\}} = C_{k,3}^{0,\{2,3\}} + B_k \log_2\left(1+\frac{\left|\mathbf{h}_{k,3}^H \mathbf{w}_{k,3}^{\{2,3\}}\right|^2}{\left|\mathbf{h}_{k,3}^H \mathbf{w}_{k,2}^{\{2,3\}}\right|^2 + B_k\sigma^2}\right), \tag{38}$$

respectively, where

$$C_{k,2}^{0,\{2,3\}} + C_{k,3}^{0,\{2,3\}} \leq \min\left\{R_{k,2}^{0,\{2,3\}}, R_{k,3}^{0,\{2,3\}}\right\} \tag{39}$$

with

$$R_{k,2}^{0,\{2,3\}} = B_k \log_2\left(1+\frac{\left|\mathbf{h}_{k,2}^H \mathbf{w}_{k,0}^{\{2,3\}}\right|^2}{\left|\mathbf{h}_{k,2}^H \mathbf{w}_{k,2}^{\{2,3\}}\right|^2 + \left|\mathbf{h}_{k,2}^H \mathbf{w}_{k,3}^{\{2,3\}}\right|^2 + B_k\sigma^2}\right) \tag{40}$$

$$R_{k,3}^{0,\{2,3\}} = B_k \log_2\left(1+\frac{\left|\mathbf{h}_{k,3}^H \mathbf{w}_{k,0}^{\{2,3\}}\right|^2}{\left|\mathbf{h}_{k,3}^H \mathbf{w}_{k,2}^{\{2,3\}}\right|^2 + \left|\mathbf{h}_{k,3}^H \mathbf{w}_{k,3}^{\{2,3\}}\right|^2 + B_k\sigma^2}\right). \tag{41}$$

5) Case 5 - User 1 Selects NR k While Users 2 and 3 Do Not: Only user 1 belongs to group k (*i.e.* $\mathcal{N}_k = \{1\}$) with the happening probability of $x_{k,1}\left(1-x_{k,2}\right)\left(1-x_{k,3}\right)$. The data rate obtained by user 1 is given by

$$R_{k,1}^{\text{tot},\{1\}} = C_{k,1}^{0,\{1\}} + B_k \log_2\left(1+\frac{\left|\mathbf{h}_{k,1}^H \mathbf{w}_{k,1}^{\{1\}}\right|^2}{B_k\sigma^2}\right) \quad (42)$$

where $C_{k,1}^{0,\{1\}} \leq R_{k,1}^{0,\{1\}}$ with $R_{k,1}^{0,\{1\}} = B_k \log_2\left(1+\frac{|\mathbf{h}_{k,1}^H \mathbf{w}_{k,0}^{\{1\}}|^2}{|\mathbf{h}_{k,1}^H \mathbf{w}_{k,1}^{\{1\}}|^2+B_k\sigma^2}\right)$.

6) Case 6 - User 2 Selects NR k While Users 1 and 3 Do Not: Only user 2 belongs to group k (*i.e.* $\mathcal{N}_k = \{2\}$) with the happening probability of $\left(1-x_{k,1}\right)x_{k,2}\left(1-x_{k,3}\right)$. The data rate obtained by user 2 is given by

$$R_{k,2}^{\text{tot},\{2\}} = C_{k,2}^{0,\{2\}} + B_k \log_2\left(1+\frac{\left|\mathbf{h}_{k,2}^H \mathbf{w}_{k,2}^{\{2\}}\right|^2}{B_k\sigma^2}\right) \quad (43)$$

where $C_{k,2}^{0,\{2\}} \leq R_{k,2}^{0,\{2\}}$ with $R_{k,2}^{0,\{2\}} = B_k \log_2\left(1+\frac{|\mathbf{h}_{k,2}^H \mathbf{w}_{k,0}^{\{2\}}|^2}{|\mathbf{h}_{k,2}^H \mathbf{w}_{k,2}^{\{2\}}|^2+B_k\sigma^2}\right)$.

7) Case 7 - User 3 Selects NR k While Users 1 and 2 Do Not: Only user 3 belongs to group k (*i.e.* $\mathcal{N}_k = \{3\}$) with the happening probability of $\left(1-x_{k,1}\right)\left(1-x_{k,2}\right)x_{k,3}$. The data rate obtained by user 3 is given by

$$R_{k,3}^{\text{tot},\{3\}} = C_{k,3}^{0,\{3\}} + B_k \log_2\left(1+\frac{\left|\mathbf{h}_{k,3}^H \mathbf{w}_{k,3}^{\{3\}}\right|^2}{B_k\sigma^2}\right) \quad (44)$$

where $C_{k,3}^{0,\{3\}} \leq R_{k,3}^{0,\{3\}}$ with $R_{k,3}^{0,\{3\}} = B_k \log_2\left(1+\frac{|\mathbf{h}_{k,3}^H \mathbf{w}_{k,0}^{\{3\}}|^2}{|\mathbf{h}_{k,3}^H \mathbf{w}_{k,3}^{\{3\}}|^2+B_k\sigma^2}\right)$.

The expected data rates achieved by users 1, 2, and 3 on the same NR k are determined by

$$\begin{aligned}\bar{R}_{k,1}^{\text{tot}} = {} & R_{k,1}^{\text{tot},\{1\}} x_{k,1}\left(1-x_{k,2}\right)\left(1-x_{k,3}\right) \\ & + R_{k,1}^{\text{tot},\{1,2\}} x_{k,1}x_{k,2}\left(1-x_{k,3}\right) \\ & + R_{k,1}^{\text{tot},\{1,3\}} x_{k,1}\left(1-x_{k,2}\right)x_{k,3} \\ & + R_{k,1}^{\text{tot},\{1,2,3\}} x_{k,1}x_{k,2}x_{k,3} \quad (45)\\ \bar{R}_{k,2}^{\text{tot}} = {} & R_{k,2}^{\text{tot},\{2\}}\left(1-x_{k,1}\right)x_{k,2}\left(1-x_{k,3}\right) \\ & + R_{k,2}^{\text{tot},\{1,2\}} x_{k,1}x_{k,2}\left(1-x_{k,3}\right) \\ & + R_{k,2}^{\text{tot},\{2,3\}}\left(1-x_{k,1}\right)x_{k,2}x_{k,3} \\ & + R_{k,2}^{\text{tot},\{1,2,3\}} x_{k,1}x_{k,2}x_{k,3} \quad (46)\end{aligned}$$

and

$$\begin{aligned}\bar{R}_{k,3}^{\text{tot}} = {} & R_{k,3}^{\text{tot},\{3\}}\left(1-x_{k,1}\right)\left(1-x_{k,2}\right)x_{k,3} \\ & + R_{k,3}^{\text{tot},\{1,3\}} x_{k,1}\left(1-x_{k,2}\right)x_{k,3} \\ & + R_{k,3}^{\text{tot},\{2,3\}}\left(1-x_{k,1}\right)x_{k,2}x_{k,3} \\ & + R_{k,3}^{\text{tot},\{1,2,3\}} x_{k,1}x_{k,2}x_{k,3}, \quad (47)\end{aligned}$$

respectively.

B. Expected Utility

We denote $v_{k,i}$ as the valuation of user i that it can obtain from downloading one unit data by selecting NR k. Since the user uses the NR from the BS, it must pay a service fee. We denote $\lambda_{k,i}$ as the price per data unit by using NR k from the BS. The utility achieved by user i is determined by

$$u_{k,i} = v_{k,i}\bar{R}_{k,i}^{\text{tot}} - \lambda_{k,i}\bar{R}_{k,i}^{\text{tot}} = \left(v_{k,i}-\lambda_{k,i}\right)\bar{R}_{k,i}^{\text{tot}} \quad (48)$$

where $\bar{R}_{k,i}^{\text{tot}}$ is defined in Section V-A.

VI. Evolutionary Game Approaches

This section presents and discusses the TEG and FEG approaches as well as their equilibrium existence and uniqueness. For ease of following the evolutionary game approaches, we define the following key terms:

- The players are the users.
- The population/group is a set of users selecting the same NR.
- The strategy of each user is to select one of the available NRs of the BS
- The utility is the expected utility defined in Section (V-B).
- The solution is the evolutionary equilibrium at which no user will change its strategy since it already receives the highest utility, given the strategies of other users.

A. Traditional Evolutionary Game (TEG)

As presented in Section V, the user selecting different NRs over time can achieve different utilities depending on the number of other users selecting the same NR and the channel condition. The average utility achieved by the user, say user i, over NRs can be determined as follows

$$\bar{u}_i = \sum_{k\in\mathcal{K}} u_{k,i}. \quad (49)$$

Then, we can formulate the TEG model as follows [15]:

$$\dot{x}_{k,i}(t) = \exp\left(\mu\right)x_{k,i}(t)\left[u_{k,i}-\bar{u}_i\right], \forall i \in \mathcal{N}_k, \forall k \in \mathcal{K} \quad (50)$$

$$\begin{aligned}R_{k,1}^{0,\{1,2,3\}} &= B_k \log_2\left(1+\frac{\left|\mathbf{h}_{k,1}^H \mathbf{w}_{k,0}^{\{1,2,3\}}\right|^2}{\left|\mathbf{h}_{k,1}^H \mathbf{w}_{k,1}^{\{1,2,3\}}\right|^2+\left|\mathbf{h}_{k,1}^H \mathbf{w}_{k,2}^{\{1,2,3\}}\right|^2+\left|\mathbf{h}_{k,1}^H \mathbf{w}_{k,3}^{\{1,2,3\}}\right|^2+B_k\sigma^2}\right) \\ R_{k,2}^{0,\{1,2,3\}} &= B_k \log_2\left(1+\frac{\left|\mathbf{h}_{k,2}^H \mathbf{w}_{k,0}^{\{1,2,3\}}\right|^2}{\left|\mathbf{h}_{k,2}^H \mathbf{w}_{k,1}^{\{1,2,3\}}\right|^2+\left|\mathbf{h}_{k,2}^H \mathbf{w}_{k,2}^{\{1,2,3\}}\right|^2+\left|\mathbf{h}_{k,2}^H \mathbf{w}_{k,3}^{\{1,2,3\}}\right|^2+B_k\sigma^2}\right) \\ R_{k,3}^{0,\{1,2,3\}} &= B_k \log_2\left(1+\frac{\left|\mathbf{h}_{k,3}^H \mathbf{w}_{k,0}^{\{1,2,3\}}\right|^2}{\left|\mathbf{h}_{k,3}^H \mathbf{w}_{k,1}^{\{1,2,3\}}\right|^2+\left|\mathbf{h}_{k,3}^H \mathbf{w}_{k,2}^{\{1,2,3\}}\right|^2+\left|\mathbf{h}_{k,3}^H \mathbf{w}_{k,3}^{\{1,2,3\}}\right|^2+B_k\sigma^2}\right). \quad (26)\end{aligned}$$

where $\dot{x}_{k,i}(t)$ is the first-order derivative of $x_{k,i}(t)$, $x_{k,i}(0)$ is the initial strategy of user i in group k, and μ is the strategy adaptation/changing rate. Equation (50) expresses that users dynamically select an NR to achieve higher utility until the game converges to an equilibrium.

To prove the existence of the TEG, we follow Theorem 1. First, we let $f_{k,i}(t, x_{k,i}) = \mu x_{k,i}(t)\left[u_{k,i}(t) - \overline{u}_i(t)\right]$, and then Equation (50) is rewritten as follows

$$\dot{x}_{k,i}(t) = f_{k,i}\left(t, x_{k,i}\right) \tag{51}$$

given the initial strategy $x_{k,i}(0)$ for all $i \in \mathcal{N}_k$, $k \in \mathcal{K}$.

Theorem 1 [41]: Problem in (51) has a unique solution if $f_{k,i}(t, x_{k,i})$ and its derivation $\partial f_{k,i}/\partial x_{k,i}$ are continuous with respect to t, $\forall t \in [0, T]$. Then, the strategy of user i selecting NR k at the $\langle z+1\rangle$-th iteration is

$$x_{k,i}^{\langle z+1\rangle}(t) = x_{k,i}\left(0\right) + \int_0^t f_{k,i}(t, x_{k,i}^{\langle z\rangle}(s))\,\mathrm{d}s. \tag{52}$$

Functions $x_{k,i}^{\langle z\rangle}(t)$ converges to the equilibrium of the game.

Proof: One effective way to prove Theorem 1 is to leverage the Banach fixed-point theorem [42], which is well presented in [41] and therefore omitted in this paper. Instead, we demonstrate that the TEG used for our system model can reach to the equilibrium. First, it is simply observed that variables $x_{k,i}(t)$, $0 \le x_{k,i}(t) \le 1$, $i \in \mathcal{N}_k$, $k \in \mathcal{K}$ are continuous respect to t. Moreover, elements of each channel vector of $\mathbf{h}_{k,i}(t)$ are continuous respect to t due to the static flat-fading channel model. Thus, the expected data rate of each user, *i.e.* $\bar{R}_{k,i}$, is continuous with respect to t. Consequently, functions $u_{k,i}(t)$ and $\overline{u}_i(t)$ are continuous at every time t. Overall, we have $f_{k,i}(t, x_{k,i})$ and $\frac{\partial f_{k,i}(t,x_{k,i})}{\partial x_{k,i}}$ are continuous. Therefore, according to Theorem 1, the TEG defined in (51) (or in (50)) is guaranteed to converge to a unique equilibrium, which will also be verified by numerical results. ∎

The TEG approach is implemented as follows. First, each user randomly selects an NR by sending a message to BS. Then, BS divides te users into groups, each of which consists of the users selecting the same NR. BS applies the RSMA scheme to each group by optimizing the common data rate and beamformers associated with the common message and private messages according to Algorithm 1. The BS then calculates the expected data rate for each user as presented in Section V-A. The data rate information is sent to the corresponding user to compute its utility according to (48). The user sends the utility information back to the BS. BS calculates the average utility of the user and sends this information to the user. The user can switch its NR selection in the next iteration to achieve a higher utility. As all users achieve the same utility by selecting any NRs, no user has an incentive to change its strategy and the TEG converges to the equilibrium.

B. Fractional Evolutionary Game (FEG)

With the TEG approach presented in Section VI-A, at time instant t, each user uses the instantaneously achievable utility functions, *i.e.* $\bar{u}_i$ and $u_{k,i}$, without their memory. The TEG approach is thus considered to be a memory-disabled economic process [43]. In this section, we first introduce the concept of memory-enabled economic process (MeEP), which is considered to be a core concept of FEG. Then, we present the use of FEG for modelling the NR selection of the users with MeEP. The FEG approach is then proven to converge to a unique equilibrium.

1) Memory-Enabled Economic Process (MeEP): We first define an MeEP. For this, we denote t as the current time instant, i.e., the time when users make their selection decisions, and $\tau \in [0, t)$ as a previous time instant. Then, MeEP is a process in which its output at the current time instant depends on the inputs at current and previous time instants [43]. In other words, the output is a function not only of the input at the current time instant but also of the input at the previous instants. To describe the MeEP, we consider an economic model that consists of an input variable, denoted by $X(t)$, and an output variable, denoted by $Z(t)$. Then, the relationship between the input and the output of the economic process is [43]

$$Z(t) = \Phi_0^t\left(X\left(\tau\right)\right) + Z\left(0\right) \tag{53}$$

where $Z\left(0\right)$ is the initial state of $Z(t)$ and $\Phi_0^t\left(X\left(\tau\right)\right)$ is given by

$$\Phi_0^t\left(X\left(\tau\right)\right) := \int_0^t \Omega_\beta\left(t-\tau\right) X\left(\tau\right) \mathrm{d}\tau \tag{54}$$

with $\Omega_\beta\left(t-\tau\right)$ being the weight to evaluate the impact of the economics process of the previous time instants on the current output. In particular, the function $\Omega_\beta(t-\tau)$ captures the memory dynamics, which has the following form [43]:

$$\Omega_\beta(t-\tau) = \frac{1}{\Gamma(\beta)(t-\tau)^{1-\beta}} \tag{55}$$

where $\Gamma\left(\cdot\right)$ is the gamma function and defined by $\Gamma\left(\beta\right) = \int_0^{+\infty} x^{\beta-1}e^{-x}\mathrm{dx}$. It can be seen from (53)-(55) that the input $X(\tau)$ has the power-law fading impact on the output $Z(t)$. In the case, we can say that the memory dynamics defined in (55) can describe the power-law fading impact of the memory on the current decision-making. To further understand the MeEP, we give a special case as an example by assuming $Z(0) = 0$ and $Z(t) = \Phi_0^t\left(X\left(\tau\right)\right)$, where $Z(0)$ is the constant and hence does not impact $Z(t)$ as $X(t)$ varies.

First, we consider the unit input variable, i.e., $X(\tau) = 1, \forall \tau \in [0, \infty)$. Then, the output of the MeEP is [43]

$$\begin{aligned} Z(t) &= \int_0^t \Omega_\beta\left(t-\tau\right) X\left(\tau\right)|_{X(\tau)=1,\forall\tau\in[0,\infty)}\,\mathrm{d}\tau \\ &= \int_0^t \Omega_\beta\left(t-\tau\right)\mathrm{d}\tau = \frac{\mathrm{t}^\beta}{\Gamma(\beta+1)} \neq \mathrm{t}. \end{aligned} \tag{56}$$

In this case, the memory dynamics defined in (55) is not a unit preserving memory. We can say that the MeEP cannot remember a constant value during the infinitely long period of time, which will decay with respect to time and is practical.

According to the Leibniz integral rule, we have

$$\frac{\mathrm{d}}{\mathrm{dt}} Z(t) = \Omega_\beta\left(0\right) X(t) + \int_0^t \left[\frac{\mathrm{d}}{\mathrm{dt}}\Omega_\beta\left(t-\tau\right)\right] X(\tau)\mathrm{d}\tau.$$

It can be observed that $Z(t)$ depends on both $X(t)$ and $X(\tau)$, and the relationship between them is considered to be the

MeEP, which is expressed by in a different way by taking the derivation of $Z(t)$ at the order of β as follows

$$ {}_0^{\mathrm{C}}D_t^{\beta} Z(t) = X(t) \tag{57}$$

with initial state of the process output $Z(0)$, where ${}_0^{\mathrm{C}}D_t^{\beta} Z(t)$ is the βth-order Caputo left-sided fractional derivative of $Z(t)$ [44] given by

$$ {}_0^{\mathrm{C}}D_t^{\beta} Z(t) = \frac{1}{\Gamma(\lceil\beta\rceil - \beta)} \int_0^t \frac{Z^{(\lceil\beta\rceil)}(\tau)}{(t-\tau)^{\beta+1-\lceil\beta\rceil}} \mathrm{d}\tau. \tag{58}$$

By incorporating the memory effect, the TEG defined in (50) becomes FEG as follows [43]:

$$ {}_0^{\mathrm{C}}D_t^{\beta} x_{k,i}(t) = \exp(\mu) x_{k,i}(t) \left[u_{k,i} - \bar{u}_i\right], \quad \forall i,k \tag{59}$$

where $x_{k,i}(0)$ is user i's initial strategy and $\beta \in (0,1)$ is the order of the fractional derivative and defined as the memory effect coefficient. With the FEG defined in (59), each user accounts its past experience as making its NR selection decision. Moreover, the past experiences at different time instances differently affect the decision-making of the user. As such, we can expect that the FEG is better than the TEG defined in (50), which will be validated by simulation results. It is notable that when $\beta = 1$, $\Omega_\beta(t-\tau)$ is a constant, which transforms the MeEP (*i.e.* FEG defined in (59)) back to the memory-disabled economic process, such as TEG defined in (50).

2) Proof of Equilibrium Existence: First, we equivalently convert the FEG defined in (59) into a problem given in (61). We then show that the existence and uniqueness of the equilibrium in (61), which is also of FEG.

By $\mathbf{X}(t) \triangleq [x_{k,i}(t)]_{i\in\mathcal{N}_k, k\in\mathcal{K}}$ and $\mathbf{E}(\mathbf{X}(t)) \triangleq \left[\exp(\mu) x_{k,i}(t)\left[u_{k,i}(t) - \bar{u}_i(t)\right]\right]_{i\in\mathcal{N}_k, k\in\mathcal{K}}$, FEG defined in (59) is then rewritten as

$$ {}_0^{\mathrm{C}}D_t^{\beta} \mathbf{X}(t) = \mathbf{E}(\mathbf{X}(t)) \tag{60}$$

where $\mathbf{X}(0) = [x_{k,i}(0)]_{i\in\mathcal{N}_k, k\in\mathcal{K}}$ is the initial strategy. We denote $e_{k,i}$ as an element of vector $\mathbf{E}$. Then, we have the following theorem:

Theorem 2: The fractional game defined in (60) can be transformed into the following equivalent problem

$$ \mathbf{X}(t) = \mathbf{X}(0) + {}_0\mathrm{I}_\mathrm{t}^{\beta}\mathbf{E}(\mathbf{X}(\mathrm{t})), \forall \mathrm{t} \in \mathcal{T} \tag{61}$$

where

$$ {}_0\mathrm{I}_\mathrm{t}^{\beta}\mathbf{E}(\mathbf{X}(\mathrm{t})) = \int_0^{\mathrm{t}} \frac{(\mathrm{t}-\tau)^{\beta-1}}{\Gamma(\beta)} \mathbf{E}(\mathbf{X}(\tau))\mathrm{d}\tau \tag{62}$$

is the fractional integral [45], if i) $e_{k,i}$ belongs to a set of the twice differentiable functions and ii) $\frac{\partial}{\partial x_{k,i}} e_{k,i}$ exists and is bounded. In particular, $\frac{\partial}{\partial x_{k,i}} e_{k,i}$ is bounded meaning that $\exists B \in \mathbb{R}^+ : |e_{k,i}(\hat{\mathbf{X}}(t)) - e_{k,i}(\tilde{\mathbf{X}}(t))| < B||(\hat{\mathbf{X}}(t)) - \tilde{\mathbf{X}}(t)||_{\mathcal{L}_1}$, which satisfies the Lipschitz condition.

Proof: We take the derivative of $\mathbf{X}(t)$ in (61) at $\lceil\beta\rceil$-th order with respect to t, and we have

$$\begin{aligned} \frac{\mathrm{d}^{\lceil\beta\rceil}}{\mathrm{dt}^{\lceil\beta\rceil}}\mathbf{X}(t) =& \frac{\mathrm{d}^{\lceil\beta\rceil}}{\mathrm{dt}^{\lceil\beta\rceil}}\left[{}_0\mathrm{I}_\mathrm{t}^{\beta}\mathbf{E}(\mathbf{X}(\mathrm{t}))\right] \\ =& {}_0^{\mathrm{RL}}D_t^{\lceil\beta\rceil-\beta}\mathbf{E}(\mathbf{X}(t)) \\ =& \frac{t^{\beta-\lceil\beta\rceil}}{\Gamma(1-\lceil\beta\rceil+\beta)}\mathbf{E}(\mathbf{X}(0)) + {}_0^{\mathrm{C}}D_t^{\beta}\mathbf{E}(\mathbf{X}(t)) \end{aligned} \tag{63}$$

with ${}_0^{\mathrm{RL}}D_t^{\beta}\mathbf{E}(\mathbf{X}(t))$ being defined as the βth-order left-sided Riemann-Liouville fractional derivative with respect to t, and the derivation in (B.1) is satisfied. For $\sigma \in (0,t)$, the $\mathcal{L}^1$ norm of $\frac{t^{\beta-\lceil\beta\rceil}}{\Gamma(1-\lceil\beta\rceil+\beta)}\mathbf{E}(\mathbf{X}(0))$ has an upper bound that is [15]

$$\begin{aligned} &\left\|\frac{t^{\beta-\lceil\beta\rceil}}{\Gamma(1-\lceil\beta\rceil+\beta)}\mathbf{E}(\mathbf{X}(0))\right\|_{\mathcal{L}^1} \\ &\qquad \le \left\|\frac{\sigma^{\beta-\lceil\beta\rceil}}{\Gamma(1-\lceil\beta\rceil+\beta)}\mathbf{E}(\mathbf{X}(0))\right\|_{\mathcal{L}^1}. \end{aligned} \tag{64}$$

Using the second condition in Theorem 2, Equation (63), (B.1) in Appendix B, and Inequality (64), we have

$$\begin{aligned} &\left\|\frac{\mathrm{d}^{\lceil\beta\rceil}}{\mathrm{dt}^{\lceil\beta\rceil}}\mathbf{X}(t)\right\|_{\mathcal{T}} \\ \le& \left\|\frac{\sigma^{\beta-\lceil\beta\rceil}}{\Gamma(1-\lceil\beta\rceil+\beta)}\mathbf{E}(\mathbf{X}(0))\right\|_{\mathcal{L}^1} + \left\|{}_0\mathrm{I}_\mathrm{t}^{\beta}\frac{\mathrm{d}^{\lceil\beta\rceil}}{\mathrm{dt}^{\lceil\beta\rceil}}\mathbf{E}(\mathbf{X}(\mathrm{t}))\right\|_{\mathcal{T}} \\ \le& \left\|\frac{\sigma^{\beta-\lceil\beta\rceil}}{\Gamma(1-\lceil\beta\rceil+\beta)}\mathbf{E}(\mathbf{X}(0))\right\|_{\mathcal{L}^1} + \left\|{}_0\mathrm{I}_\mathrm{t}^{\beta}\frac{\mathrm{d}^{\lceil\beta\rceil}}{\mathrm{dt}^{\lceil\beta\rceil}}\mathbf{X}(\mathrm{t})\right\|_{\mathcal{T}}\mathrm{AB} \end{aligned} \tag{65}$$

where $\|z\|_{\mathcal{T}} \triangleq \int_{\mathcal{T}} \exp(-\mu t)\|z\|_{\mathcal{L}^1}\mathrm{dt}$ and A is the cardinality of $\{(i,k)|\, i \in \mathcal{N}_k, k \in \mathcal{K}\}$. For the last term in (65), we have (B.2). Then, substituting (B.2) into (65), we have

$$\begin{aligned} &\left\|\frac{\mathrm{d}^{\lceil\beta\rceil}}{\mathrm{dt}^{\lceil\beta\rceil}}\mathbf{X}(t)\right\|_{\mathcal{T}} \\ \le& \left\|\frac{\sigma^{\beta-\lceil\beta\rceil}}{\Gamma(1-\lceil\beta\rceil+\beta)}\mathbf{E}(\mathbf{X}(0))\right\|_{\mathcal{L}^1} + \frac{AB}{\mu^{\beta}}\left\|\frac{\mathrm{d}^{\lceil\beta\rceil}}{\mathrm{ds}^{\lceil\beta\rceil}}\mathbf{X}(t)\right\|_{\mathcal{T}} \\ \Leftrightarrow& \left\|\frac{\mathrm{d}^{\lceil\beta\rceil}}{\mathrm{dt}^{\lceil\beta\rceil}}\mathbf{X}(t)\right\|_{\mathcal{T}} \le \frac{1}{1-\frac{AB}{\mu^{\beta}}}\left\|\frac{\sigma^{\beta-\lceil\beta\rceil}}{\Gamma(1-\lceil\beta\rceil+\beta)}\mathbf{E}(\mathbf{X}(0))\right\|_{\mathcal{L}^1}. \end{aligned} \tag{66}$$

As observed from (66), given a large value of μ, $\frac{AB}{\mu^{\beta}} < 1$ and $\left\|\frac{\mathrm{d}^{\lceil\beta\rceil}}{\mathrm{dt}^{\lceil\beta\rceil}}\mathbf{X}(t)\right\|_{\mathcal{T}}$ is bounded. In this case, we can take the fractional derivative of $\mathbf{X}(t)$ with an order of $\beta \in (0,1)$ as follows:

$$\begin{aligned} {}_0^{\mathrm{C}}D_t^{\beta}\mathbf{X}(t) =& {}_0\mathrm{I}_\mathrm{t}^{\lceil\beta\rceil-\beta}\frac{\mathrm{d}^{\lceil\beta\rceil}}{\mathrm{dt}^{\lceil\beta\rceil}}\mathbf{X}(\mathrm{t}) \\ =& {}_0\mathrm{I}_\mathrm{t}^{\lceil\beta\rceil-\beta}\Big\{\frac{\mathrm{t}^{\beta-\lceil\beta\rceil}}{\Gamma(1-\lceil\beta\rceil+\beta)}\mathbf{E}(\mathbf{X}(0)) \\ &+ {}_0\mathrm{I}_\mathrm{t}^{\beta}\Big[\frac{\mathrm{d}^{\lceil\beta\rceil}}{\mathrm{dt}^{\lceil\beta\rceil}}\mathbf{E}(\mathbf{X}(\mathrm{t}))\Big]\Big\} \\ =& \mathbf{E}(\mathbf{X}(t)). \end{aligned} \tag{67}$$

The derivation in (67) clearly shows that the game in (60) is equivalent to that given in (61). Therefore, The proof of Theorem 2 is completed. ■

Now, we prove the uniqueness of the solution to the problem defined in (61). Indeed, denote F as an operator, $F : \mathcal{D}_{\mathbf{X}} \mapsto \mathcal{D}_{\mathbf{X}}$, where $\mathcal{D}_{\mathbf{X}}$ is the feasible domain of $\mathbf{X}$. Then, based on (B.3), we have

$$\left\|F\hat{\mathbf{X}}(t) - F\tilde{\mathbf{X}}(t)\right\|_{\mathcal{T}} < \frac{AB}{\mu^{\beta}}\left\|\hat{\mathbf{X}}(t) - \tilde{\mathbf{X}}(t)\right\|_{\mathcal{T}}. \tag{68}$$

TABLE II
SIMULATION PARAMETERS

Parameter	Value	Parameter	Value
L	3	N	3
K	2	B_k	$12 \times 15 \times 2$ kHz
μ	-2	$\lambda_{k,i}$	5×10^{-7}
$v_{k,i}$	10^{-6}	P_k	26dBm
β	$\{0.7, 0.8, 0.9, 1\}$	σ^2	-174 dBm/Hz

Moreover, $\left\|F\hat{\mathbf{X}}(t) - F\tilde{\mathbf{X}}(t)\right\|_{\mathcal{T}} < \left\|\hat{\mathbf{X}}(t) - \tilde{\mathbf{X}}(t)\right\|_{\mathcal{T}}$ if $\mu^\beta \geq AB$. In this case, F satisfies the fixed point theorem implying the uniqueness of the solution to (61).

3) Stability of the Solution to the FEG: We leverage (68) to prove the stability of the solution to the FEG. Indeed, we assume that $\hat{\mathbf{X}}(0) \triangleq [\hat{x}_{k,i}(0)]_{i\in\mathcal{N}_k, k\in\mathcal{K}}$ and $\tilde{\mathbf{X}}(0) \triangleq [\tilde{x}_{k,i}(0)]_{i\in\mathcal{N}_k, k\in\mathcal{K}}$ are two different initial states that satisfy $\left\|\hat{\mathbf{X}}(0) - \tilde{\mathbf{X}}(0)\right\|_{\mathcal{L}^1} \leq \varphi$. Furthermore, we denote $\hat{\mathbf{X}}(t)$ and $\tilde{\mathbf{X}}(t)$, for all t are the solutions to the FEG corresponding to $\hat{\mathbf{X}}(0)$ and $\tilde{\mathbf{X}}(0)$, respectively. Then, based on (68), we have the following inequality:

$$\begin{aligned}\left\|\hat{\mathbf{X}}(t) - \tilde{\mathbf{X}}(t)\right\|_{\mathcal{T}} &< \frac{AB}{\mu^\beta}\left\|\hat{\mathbf{X}}(0) - \tilde{\mathbf{X}}(0)\right\|_{\mathcal{L}^1} \\ &< \frac{AB}{\mu^\beta}\varphi \triangleq \epsilon. \end{aligned} \tag{69}$$

The inequality given in (69) implies the stability for the solution to the FEG if and only if $\frac{AB}{\mu^\beta} < 1$.

The implementation steps of the FEG approach are similar to those of the TEG approach. The difference is that each user makes its NR decision based on the returned average utility and its previous decision, which is stored in the user's memory storage.

VII. PERFORMANCE EVALUATION

In this section, we provide simulation results to validate the game approaches. The game approach with $\beta = 1$ corresponds to the TEG approach, while the game with $\beta < 1$ corresponds to the FEG approach. In particular for the FEG approaches, we consider the cases of $\beta = 0.9, 0.8$ and 0.7. The users are uniformly distributed in a square area of 300 m $\times$ 300 m, and the BS is placed at the center of area and at a height of 10 m above the ground level. The channel corresponding to NR k from the BS to user i is $\sqrt{10^{\gamma_{\text{PL},i}/10}}\bar{\mathbf{h}}_{k,i}$, where $\gamma_{\text{PL},i} = 30 + 2.2\log(d_i)$ is the large-scale fading with d_i being the distance (in meter) between the BS and the user, and $\bar{\mathbf{h}}_{k,i} \sim \mathcal{CN}(0, \mathbf{I})$ is the Rayleigh fading channel. Other simulation parameters are provided in Table II [31].

First, it is important to discuss how the NR selection strategies change over evolutionary time, which are illustrated in Figs. 2(a), (b) and (c). As can be seen that the strategies of the users selecting different NRs of both TEG and FEG approaches are able to converge to an equilibrium point over time. This results validate the equilibrium existence of the games. In addition, the strategies of the users as the evolutionary games with higher values of β converge to the equilibrium faster. To evaluate the effectiveness of the proposed game,

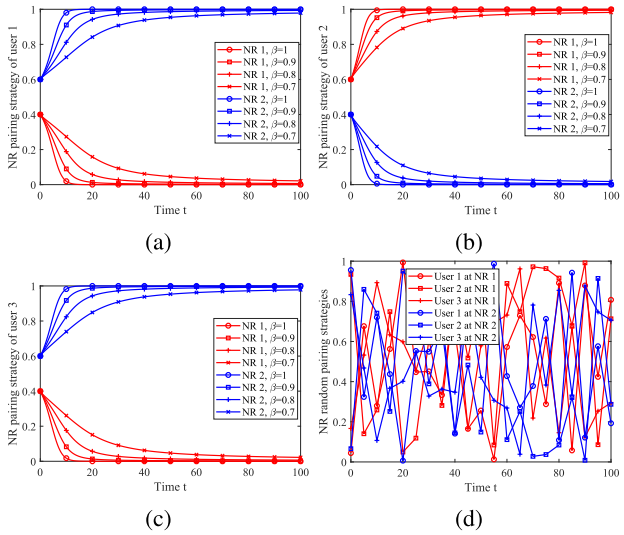

Fig. 2. Proportion of users selecting different NRs.

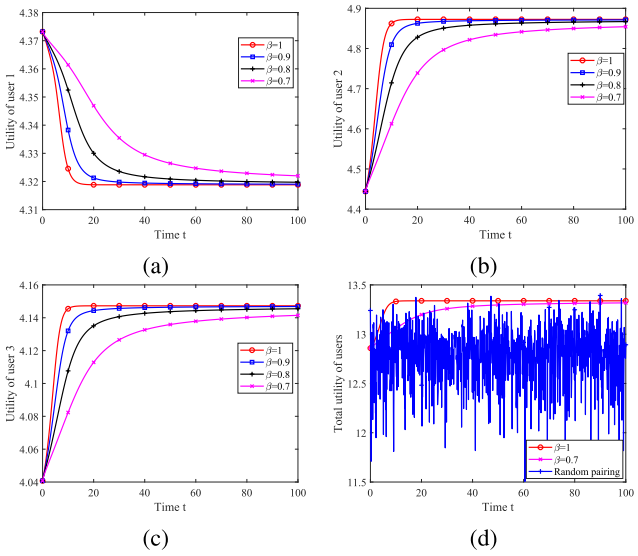

Fig. 3. The users' utilities.

we introduce the random pairing method as a baseline scheme in which at each time step, each user randomly selects one of the available NRs of the BS. With the random pairing scheme, as shown in Fig. 2 (d), the users' strategies show a large fluctuation and do not converge to the equilibrium. To further verify these results, we show the utilities obtained by users 1, 2 and 3 over time in Fig. 3(a), (b) and (c), respectively. As observed from these figures, as β decreases, the convergence speed of the users' utilities is slower. The reason is that with a low value of β (e.g., $\beta = 0.7$), the memory effects become more important in the decision-making of the users, meaning that users will adapt more slowly and cautiously. Fig. 3(d) shows the sum utility obtained by the proposed game approaches and the baseline scheme. As seen, the users' sum utility largely fluctuates over time steps. This means that at any time step, users may not know their utilities obtained in the next time step. Moreover, the proposed game approaches offer the higher sum utility, compared to the baseline scheme. These

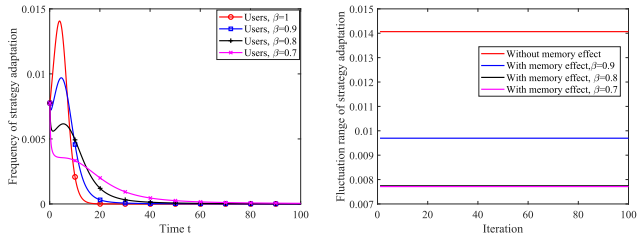

(a) (b)

Fig. 4. (a) The frequency of strategy adaptation (b) the range of the strategy adaption of the users.

results clearly demonstrate that our proposed game approaches outperform the baseline scheme in terms of stability and utility.

Fig. 4(a) shows the strategy adaptation frequency of the users with different values of β, and Fig. 4(b) shows the fluctuation range of the strategy adaptation of the users. Thus, Figs. 4(a) and (b) have the same phenomenon. As observed from Fig. 4(a), the users' strategy adaptation fluctuates less as β decreases. This implies that users with a low value of β have less re-activeness, resulting in the slower convergence speed of the users.

An important question is that how we benefit the less re-activeness and low strategy adaptation frequency of the users? In other words, is the FEG approach better than TEG approach? Indeed, the strategy adaptation frequency of the users is lower, meaning that users will switch among the NRs less often. Thus, BS spends less computing and communication resources (*i.e.* performing the channel estimation and optimizing beamformers) to establish communications of the users. Therefore, in the terms of network resource cost, the FEG approach is better than the TEG approach.

Next, we discuss the stability of the users' strategies, which is represented by the direction field of the replicator dynamics in Figs. 5(a), (b) and (c). In these figures, we use the strategy pairs (i.e., $x_{1,1}$ and $x_{2,2}$, $x_{1,2}$ and $x_{2,3}$, and $x_{2,1}$ and $x_{1,3}$) to show the stability of the solution. Moreover, the red star marks the equilibrium state of the games, and the the blue rows represent strategy adaptations of the users. As seen, the blue rows in the FEG ultimately reach and stabilize at the optimal solution, i.e., the red star. The results shown in Figs. 5(a), (b) and (c) verify the robustness and stability of the solution to the evolutionary game approaches.

We now investigate the impact of the number of available NRs K on the total utility obtained by users. As shown in Fig. 6(a), as K increases, the total utility of the users increases. The reason is that users have more NRs to select, resulting in higher possibilities to find an NR that leads to its high expected data rate and utility. This is further verified in Fig. 6(b), (c) and (d) in the case of $K = 3$ users, where each user selects one NR. Users perform the NR selection to avoid the interference caused by other users. This is reasonable in the real-world scenarios. That is, each player typically selects the strategy to avoid interest conflict with others.

Next, we discuss how the number of users in the network impacts the utility of each of them and the total utility of all users. Without loss of generality, the utility obtained by user 1 is considered. As shown in Fig. 7, the utility of user 1 seems

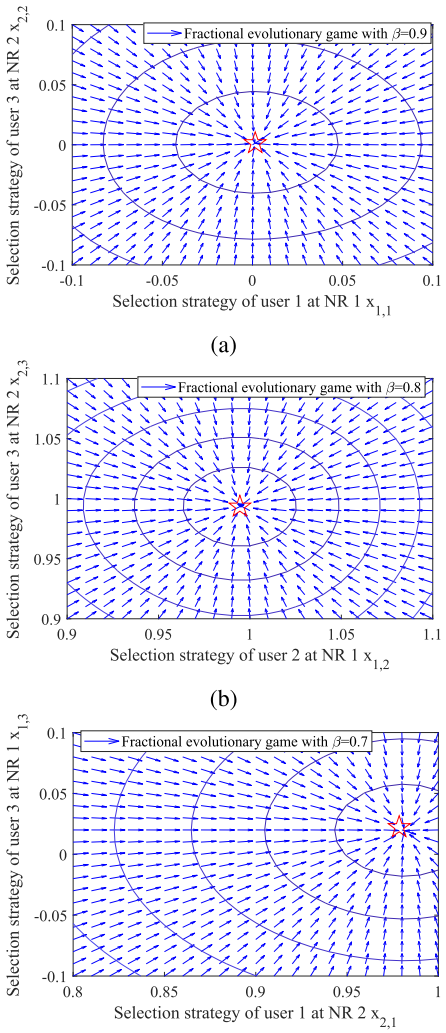

(a)

(b)

(c)

Fig. 5. The solution stability of the population game.

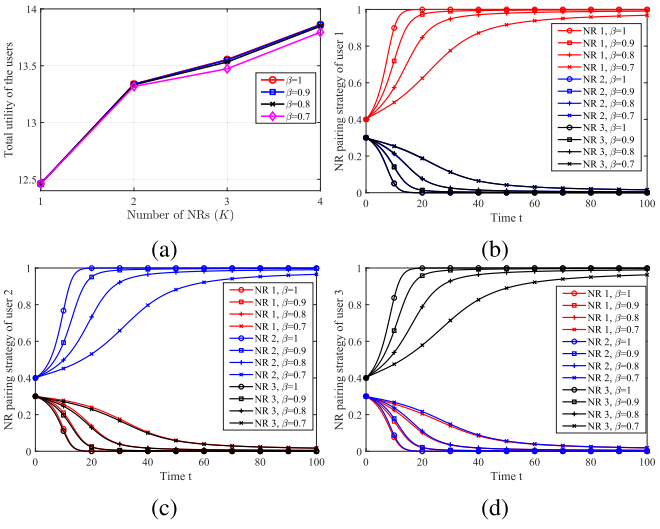

(a) (b)

(c) (d)

Fig. 6. (a) The total utility of the users vs. the number of NRs, and (b), (c) and (d) the proportions of users 1, 2, and 3 selecting different NRs in the case of $K = 3$ NRs.

to be unchanged. The reason is that the BS has two NRs, thus user 1 is always be able to find one NR that user 2 does not

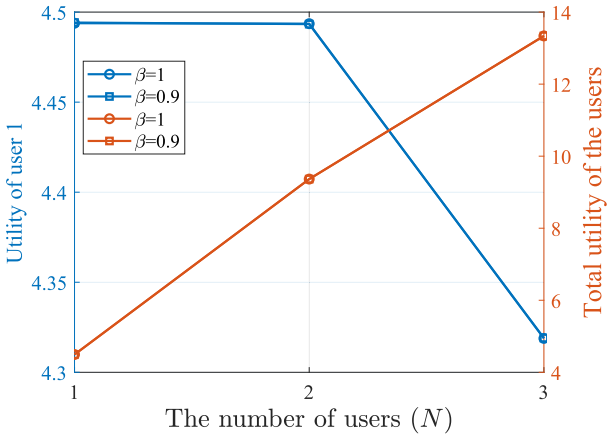

Fig. 7. The utility of user 1 and total utility of the users vs. the number of users.

select. For example, as user 2 selects NR 1, user 1 will select NR 2. Therefore, the utility of user 1 is the same in these two cases. However, as the number of users is 3, the utility of user 1 decreases. This is due to the fact that as the user 1 can select any NR, there are four possible cases for the other two users. This reduces the expected data rate achieved by user 1 and leads to the reduced utility of user 1. Fig. 7 further shows that the total utility of the users increases with the increase of the number of users. This is due to the fact that the RSMA scheme can appropriately determine the power splitting of each user to achieve the theoretically maximal rate region, which results in increasing the total utility of users.

The aforementioned results clearly demonstrate that both TEG and FEG are able to converge to the equilibrium. Note that at each time t, the users need information of the average utility broadcast by the BS to make its NR selection. However, in some scenarios with bad channel quality, the information may not be available to the users at time t. Thus, two questions are that (i) is it possible for the users to leverage the information in the past, *i.e.* $t-\delta$ with δ being the number of units of time?, and (ii) what is the maximum value of δ that the users can use for their decisions while guaranteeing the convergence?. We show the simulation results to answer these questions. First, we reformulate the replicator dynamic process of TEG and FEG by incorporating δ as follows

$$\begin{aligned} \dot{x}_{k,i}(t) &= \exp(\mu) x_{k,i}(t-\delta)\left[u_{k,i}(t-\delta) - \bar{u}_i(t-\delta)\right] \\ {}_0^{\mathrm{C}}D_t^{\beta} x_{k,i}(t) &= \exp(\mu) x_{k,i}(t-\delta)\left[u_{k,i}(t-\delta) - \bar{u}_i(t-\delta)\right] \end{aligned} \tag{70}$$

for all $i \in \mathcal{N}_k$, $k \in \mathcal{K}$. We then discuss how the delay value of δ impacts on the equilibrium of the TEG and FEG approaches. Without loss of generality, we consider the pairing strategy of user 1 at NR 1 as the TEG is used (Fig. 8(a)) and the FEG approach is used (Figs. 8(b) and (c)). As observed from Fig. 8(a), the decision-making process of user 1 fluctuates as the delay information changes at $\delta > 0$. In particular, as δ is small, *i.e.* $\delta = 15$, the strategy of user 1 (and TEG)still converges to the equilibrium. However, as δ is large, *i.e.* $\delta = 30$, TEG does not converge to the equilibrium. These results imply that as exploiting the "fresh" information

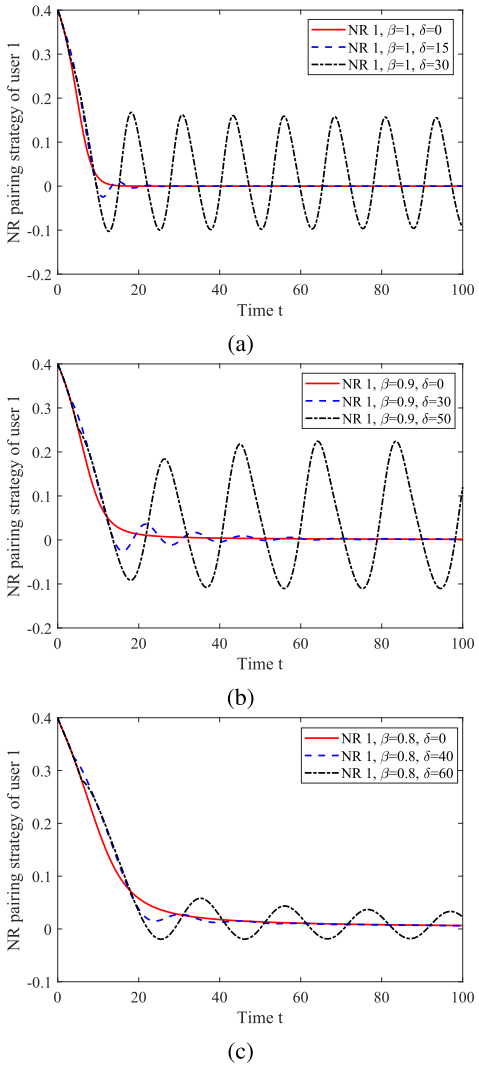

Fig. 8. Proportion of user 1 select NR 1 with different delay values.

with the small delay, *i.e.* $\delta < 30$, the game still reaches to the convergence. As δ is higher, the strategy adaptation of the users has larger fluctuations, and the game reaches the equilibrium more slowly. We can say that the game is difficult to converge to the equilibrium as the users leverages older information. To verify the robustness of the FEG schemes, Fig. 8(b) and (c) show the convergence of user 1's strategy with the cases of $\beta = 0.8$ and 0.9. As seen, the FEG scheme with $\beta = 0.9$ and $\beta = 0.8$ is able to converge to the equilibrium with a delay value of 50 and 60. Compared with the TEG, the FEG scheme allows users to leverage much older information for their decisions. In this case, we say that the FEG scheme is more robust than the TEG scheme.

VIII. Conclusion

In this paper, we have addressed the dynamic NR selection problem in the RSMA-enabled network. Specifically, users in RSMA-enabled networks are able to dynamically select different NRs over time to achieve its higher utility. We have developed the SCA-based iterative algorithm to design the optimal beamformers of the common and private messages for

the users in the same group. To model the NR adaptation of the users, we have leveraged two game approaches, *namely* TEG and FEG. In particular with the FEG approach, the memory effect (*i.e.* the past experience) of the users has been taken into account their decision-making. We have proven the unique and stable solution to the evolutionary game approaches. Both the theoretical analysis and simulation results have validated the equilibrium and the stability of the solution of the game approaches. Simulation results further show that the FEG approach outperforms the TEG approach in terms of adaptation strategy rate. This means that with the FEG approach, the BS requires less computing and computing resources (e.g. optimizing beamformers of the RSMA), since users have low frequency of NR selection. They further confirm that with the fraction game, users are able to exploit older information for their decision-making.

APPENDIX A
FUNDAMENTAL INEQUALITIES

We first consider function $f(x) = \log_2(1+1/x)$. Given $x>0$, this function is simply proved to be convex by taking the second derivative. Moreover, with $\bar{x}>0$, based on the first-order Taylor approximation, we have [46] and [47]

$$\begin{aligned} f(x) =& \log_2\left(1+\frac{1}{x}\right) \\ \geq& \log_2\left(1+\frac{1}{\bar{x}}\right) + \left.\frac{\partial f(x)}{\partial x}\right|_{x=\bar{x}}(x-\bar{x}) \\ =& \log_2\left(1+\frac{1}{\bar{x}}\right) + \frac{1}{\ln 2\,(1+\bar{x})}\left(1-\frac{x}{\bar{x}}\right). \end{aligned} \tag{A.1}$$

Now, we consider function $f(x,y) = \log_2\left(1+\frac{1}{xy}\right)$ that is also simply proven to be convex in the domain $(x>0, y>0)$. Therefore, it follows that [46]

$$\begin{aligned} f(x,y) =& \log_2\left(1+\frac{1}{xy}\right) \\ \geq& f(\bar{x},\bar{y}) + \langle \nabla f(\bar{x},\bar{y}), (x,y)-(\bar{x},\bar{y})\rangle \\ =& \log_2(1+1/\bar{x}\bar{y}) + \frac{1/\bar{x}\bar{y}}{\ln 2\,(1+1/\bar{x}\bar{y})}\left(2-\frac{x}{\bar{x}}-\frac{y}{\bar{y}}\right) \end{aligned} \tag{A.2}$$

for $x>0$, $y>0$, $\bar{x}>0$, and $\bar{y}>0$. By substituting $x \to 1/x$ and $\bar{x} \to 1/\bar{x}$, we have

$$\begin{aligned} \log_2\left(1+\frac{x}{y}\right) \geq& \log_2(1+\bar{x}/\bar{y}) + \frac{\bar{x}/\bar{y}}{\ln 2\,(1+\bar{x}/\bar{y})} \\ & \times\left(2-\frac{\bar{x}}{x}-\frac{y}{\bar{y}}\right). \end{aligned} \tag{A.3}$$

APPENDIX B
UPPERBOUNDS

First, we can show that

$$\begin{aligned} & {}_0^{\mathrm{RL}}D_t^{\lceil\beta\rceil-\beta}\mathbf{E}(\mathbf{X}(t)) \\ =& \frac{1}{\Gamma(1-\lceil\beta\rceil+\beta)}\frac{\mathrm{d}}{\mathrm{d}t}\int_0^t \frac{\mathbf{E}(\mathbf{X}(\tau))}{(t-\tau)^{\lceil\beta\rceil-\beta}}\mathrm{d}\tau \\ =& \frac{1}{\Gamma(1-\lceil\beta\rceil+\beta)}\frac{\mathrm{d}}{\mathrm{d}t}\int_0^t \theta^{\beta-\lceil\beta\rceil}\mathbf{E}(\mathbf{X}(t-\theta))\mathrm{d}\theta \\ =& \frac{1}{\Gamma(1-\lceil\beta\rceil+\beta)}\Big[t^{\beta-\lceil\beta\rceil}\mathbf{E}(\mathbf{X}^0) + \int_0^t \theta^{\beta-\lceil\beta\rceil} \\ & \times \frac{\mathrm{d}}{\mathrm{d}t}\mathbf{E}(\mathbf{X}(t-\theta))\mathrm{d}\theta\Big] \\ =& \frac{1}{\Gamma(1-\lceil\beta\rceil+\beta)}\Big[t^{\beta-\lceil\beta\rceil}\mathbf{E}(\mathbf{X}^0) + \int_0^t (t-\tau)^{\beta-\lceil\beta\rceil} \\ & \times \frac{\mathrm{d}}{\mathrm{d}\tau}\mathbf{E}(\mathbf{X}(\tau))\mathrm{d}\tau\Big] \\ =& \frac{t^{\beta-\lceil\beta\rceil}}{\Gamma(1-\lceil\beta\rceil+\beta)}\mathbf{E}(\mathbf{X}^0) + {}_0\mathrm{I}_\mathrm{t}^\beta\Big[\frac{\mathrm{d}^{\lceil\beta\rceil}}{\mathrm{dt}^{\lceil\beta\rceil}}\mathbf{E}(\mathbf{X}(\mathrm{t}))\Big]. \end{aligned} \tag{B.1}$$

In addition, it follows that [15]

$$\begin{aligned} & \Big\|{}_0\mathrm{I}_\mathrm{t}^\beta\frac{\mathrm{d}^{\lceil\beta\rceil}}{\mathrm{dt}^{\lceil\beta\rceil}}\mathbf{X}(\mathrm{t})\Big\|_{\mathcal{T}} \\ &= \int_0^T \exp(-\mu t)\Big\|{}_0\mathrm{I}_\mathrm{t}^\beta\frac{\mathrm{d}^{\lceil\beta\rceil}}{\mathrm{dt}^{\lceil\beta\rceil}}\mathbf{X}(\mathrm{t})\Big\|\mathrm{dt} \\ &\leq \int_0^T \exp(-\mu t)\int_0^t \frac{\|\frac{\mathrm{d}^{\lceil\beta\rceil}}{\mathrm{ds}^{\lceil\beta\rceil}}\mathbf{X}(s)\|}{(t-s)^{1-\beta}\Gamma(\beta)}\mathrm{ds}\mathrm{dt} \\ &= \int_0^T \frac{\exp(-\mu s)}{\Gamma(\beta)}\Big\|\frac{\mathrm{d}^{\lceil\beta\rceil}}{\mathrm{ds}^{\lceil\beta\rceil}}\mathbf{X}(s)\Big\| \\ &\quad\times\int_s^T \exp(-\mu(t-s))(t-s)^{\beta-1}\mathrm{dt}\mathrm{ds} \\ &= \int_0^T \frac{\exp(-\mu s)}{\Gamma(\beta)}\Big\|\frac{\mathrm{d}^{\lceil\beta\rceil}}{\mathrm{ds}^{\lceil\beta\rceil}}\mathbf{X}(s)\Big\| \\ &\quad\times\int_0^{\mu(T-s)} \exp(-\Psi)(\frac{\Psi}{\mu})^{\beta-1}\mathrm{d}(\frac{\Psi}{\mu})\mathrm{ds} \\ &< \frac{1}{\mu^\beta\Gamma(\beta)}\int_0^T \exp(-\mu s)\Big\|\frac{\mathrm{d}^{\lceil\beta\rceil}}{\mathrm{ds}^{\lceil\beta\rceil}}\mathbf{X}(s)\Big\|\mathrm{ds} \\ &\quad\times\int_0^{+\infty} \exp(-\Psi)\Psi^{\beta-1}\mathrm{d}\Psi \\ &= \frac{1}{\mu^\beta}\|\frac{\mathrm{d}^{\lceil\beta\rceil}}{\mathrm{ds}^{\lceil\beta\rceil}}\mathbf{X}(t)\|_{\mathcal{T}} \end{aligned} \tag{B.2}$$

and

$$\begin{aligned} & \|F\hat{\mathbf{X}}(t)-F\tilde{\mathbf{X}}(t)\|_{\mathcal{T}} \\ &= \int_0^T \exp(-\mu t)\,\|{}_0\mathbf{I}_t^\beta\mathbf{E}(\hat{\mathbf{X}}(t)) - {}_0\mathbf{I}_t^\beta\mathbf{E}(\tilde{\mathbf{X}}(t))\|\mathrm{dt} \\ &< AB\Big[\int_0^T \exp(-\mu t)\,\|{}_0\mathbf{I}_t^\beta\hat{\mathbf{X}}(t) - {}_0\mathbf{I}_t^\beta\tilde{\mathbf{X}}(t)\|\mathrm{dt}\Big] \\ &\leq AB\Big[\int_0^T \exp(-\mu t)\int_0^t \frac{\|\hat{\mathbf{X}}(s)-\tilde{\mathbf{X}}(s)\|}{\Gamma(\beta)(t-s)^{1-\beta}}\mathrm{d}s\mathrm{d}t\Big] \\ &= \frac{AB}{\Gamma(\beta)}\Big[\int_0^T\int_s^T \exp(-\mu t)\frac{\|\hat{\mathbf{X}}(s)-\tilde{\mathbf{X}}(s)\|}{(t-s)^{1-\beta}}\mathrm{dt}\mathrm{ds}\Big] \\ &= \frac{AB}{\Gamma(\beta)}\Big[\int_0^T \exp(-\mu s)\,\|\hat{\mathbf{X}}(s)-\tilde{\mathbf{X}}(s)\| \\ &\quad\times\int_s^T \frac{\exp(-\mu(t-s))}{(t-s)^{1-\beta}}\mathrm{d}s\mathrm{d}t\Big] \\ &= \frac{AB}{\mu^\beta\Gamma(\beta)}\Big[\int_0^T \exp(-\mu s)\,\|\hat{\mathbf{X}}(s)-\tilde{\mathbf{X}}(s)\| \\ &\quad\times\int_0^{\mu(T-s)} \exp(-\psi)\psi^{\beta-1}\mathrm{d}\psi\mathrm{d}s\Big] \end{aligned}$$

$$< \frac{AB}{\mu^{\beta}\Gamma(\beta)} \|\hat{\mathbf{X}}(t) - \tilde{\mathbf{X}}(t)\|_{\mathcal{T}} \int_0^{+\infty} \exp(-\sigma)\, \sigma^{\beta-1} \mathrm{d}\sigma$$
$$= \frac{AB}{\mu^{\beta}} \|\hat{\mathbf{X}}(t) - \tilde{\mathbf{X}}(t)\|_{\mathcal{T}}. \quad \text{(B.3)}$$

REFERENCES

[1] O. Dizdar, Y. Mao, W. Han, and B. Clerckx, "Rate-splitting multiple access: A new frontier for the PHY layer of 6G," in *Proc. IEEE 92nd Veh. Technol. Conf. (VTC-Fall)*, Nov. 2020, pp. 1–7.

[2] Y. Mao, O. Dizdar, B. Clerckx, R. Schober, P. Popovski, and H. V. Poor, "Rate-splitting multiple access: Fundamentals, survey, and future research trends," *IEEE Commun. Surveys Tuts.*, vol. 24, no. 4, pp. 2073–2126, 4th Quart., 2022.

[3] B. Clerckx, H. Joudeh, C. Hao, M. Dai, and B. Rassouli, "Rate splitting for MIMO wireless networks: A promising PHY-layer strategy for LTE evolution," *IEEE Commun. Mag.*, vol. 54, no. 5, pp. 98–105, May 2016.

[4] Y. Mao, B. Clerckx, and V.O. K. Li, "Energy efficiency of rate-splitting multiple access, and performance benefits over SDMA and NOMA," in *Proc. 15th Int. Symp. Wireless Commun. Syst. (ISWCS)*, Aug. 2018, pp. 1–5.

[5] B. Clerckx et al., "Rate-splitting unifying SDMA, OMA, NOMA, and multicasting in MISO broadcast channel: A simple two-user rate analysis," *IEEE Wireless Commun. Lett.*, vol. 9, no. 3, pp. 349–353, Mar. 2020.

[6] Y. Mao, B. Clerckx, and V. Li, "Rate-splitting multiple access for downlink communication systems: Bridging, generalizing, and outperforming SDMA and NOMA," *EURASIP J. Wireless Commun. Netw.*, vol. 2018, no. 1, pp. 1–54, May 2018.

[7] Y. Mao, B. Clerckx, and V.O. K. Li, "Rate-splitting multiple access for coordinated multi-point joint transmission," in *Proc. IEEE Int. Conf. Commun. Workshops (ICC Workshops)*, May 2019, pp. 1–6.

[8] A. A. Ahmad, J. Kakar, R.-J. Reifert, and A. Sezgin, "UAV-assisted C-RAN with rate splitting under base station breakdown scenarios," in *Proc. IEEE Int. Conf. Commun. Workshops (ICC Workshops)*, May 2019, pp. 1–6.

[9] H. Joudeh and B. Clerckx, "Rate-splitting for max-min fair multigroup multicast beamforming in overloaded systems," *IEEE Trans. Wireless Commun.*, vol. 16, no. 11, pp. 7276–7289, Nov. 2017.

[10] D. Yu, J. Kim, and S.-H. Park, "An efficient rate-splitting multiple access scheme for the downlink of C-RAN systems," *IEEE Wireless Commun. Lett.*, vol. 8, no. 6, pp. 1555–1558, Dec. 2019.

[11] B. Matthiesen, Y. Mao, P. Popovski, and B. Clerckx, "Globally optimal beamforming for rate splitting multiple access," in *Proc. IEEE Int. Conf. Acoust., Speech Signal Process. (ICASSP)*, Jun. 2021, pp. 4775–4779.

[12] J. Hofbauer and K. Sigmund, "Evolutionary game dynamics," *Bull. Amer. Math. Soc.*, vol. 40, no. 4, pp. 479–519, 2003.

[13] D. Niyato and E. Hossain, "Dynamics of network selection in heterogeneous wireless networks: An evolutionary game approach," *IEEE Trans. Veh. Technol.*, vol. 58, no. 4, pp. 2008–2017, May 2009.

[14] X. Gao, S. Feng, D. Niyato, P. Wang, K. Yang, and Y.-C. Liang, "Dynamic access point and service selection in backscatter-assisted RF-powered cognitive networks," *IEEE Internet Things J.*, vol. 6, no. 5, pp. 8270–8283, Oct. 2019.

[15] N. T. T. Van et al., "Dynamic network service selection in intelligent reflecting surface-enabled wireless systems: Game theory approaches," *IEEE Trans. Wireless Commun.*, vol. 21, no. 8, pp. 5947–5961, Aug. 2022.

[16] N. Luong, T. T. V. Nguyen, S. Feng, H. T. Nguyen, T. D. Niyato, and D. I. Kim, "Dynamic network service selection in IRS-assisted wireless networks: A game theory approach," *IEEE Trans. Veh. Technol.*, vol. 70, no. 5, pp. 5160–5165, May 2021.

[17] B. R. Marks and G. P. Wright, "A general inner approximation algorithm for nonconvex mathematical programs," *Oper. Res.*, vol. 26, no. 4, pp. 681–683, 1978.

[18] Z. Yang, M. Chen, W. Saad, and M. Shikh-Bahaei, "Optimization of rate allocation and power control for rate splitting multiple access (RSMA)," *IEEE Trans. Commun.*, vol. 69, no. 9, pp. 5988–6002, Sep. 2021.

[19] H. Joudeh and B. Clerckx, "Sum-rate maximization for linearly precoded downlink multiuser MISO systems with partial CSIT: A rate-splitting approach," *IEEE Trans. Commun.*, vol. 64, no. 11, pp. 4847–4861, Nov. 2016.

[20] C. Hao, Y. Wu, and B. Clerckx, "Rate analysis of two-receiver MISO broadcast channel with finite rate feedback: A rate-splitting approach," *IEEE Trans. Commun.*, vol. 63, no. 9, pp. 3232–3246, Sep. 2015.

[21] H. Joudeh and B. Clerckx, "Robust transmission in downlink multiuser MISO systems: A rate-splitting approach," *IEEE Trans. Signal Process.*, vol. 64, no. 23, pp. 6227–6242, Dec. 2016.

[22] L. Yin, B. Clerckx, and Y. Mao, "Rate-splitting multiple access for multi-antenna broadcast channels with statistical CSIT," in *Proc. IEEE Wireless Commun. Netw. Conf. Workshops (WCNCW)*, Mar. 2021, pp. 1–6.

[23] H. Chen, D. Mi, B. Clerckx, Z. Chu, J. Shi, and P. Xiao, "Joint power and subcarrier allocation optimization for multigroup multicast systems with rate splitting," *IEEE Trans. Veh. Technol.*, vol. 69, no. 2, pp. 2306–2310, Feb. 2020.

[24] L. Yin and B. Clerckx, "Rate-splitting multiple access for multibeam satellite communications," in *Proc. IEEE Int. Conf. Commun. Workshops (ICC Workshops)*, Jun. 2020, pp. 1–6.

[25] Y. Mao, B. Clerckx, and V.O. K. Li, "Rate-splitting for multi-user multi-antenna wireless information and power transfer," in *Proc. IEEE 20th Int. Workshop Signal Process. Adv. Wireless Commun. (SPAWC)*, Jul. 2019, pp. 1–5.

[26] Z. Yang, J. Shi, Z. Li, M. Chen, W. Xu, and M. Shikh-Bahaei, "Energy efficient rate splitting multiple access (RSMA) with reconfigurable intelligent surface," in *Proc. IEEE Int. Conf. Commun. Workshops (ICC Workshops)*, Jun. 2020, pp. 1–6.

[27] A. Bansal, K. Singh, B. Clerckx, C.-P. Li, and M.-S. Alouini, "Rate-splitting multiple access for intelligent reflecting surface aided multi-user communications," *IEEE Trans. Veh. Technol.*, vol. 70, no. 9, pp. 9217–9229, Sep. 2021.

[28] O. Dizdar, A. Kaushik, B. Clerckx, and C. Masouros, "Energy efficient dual-functional radar-communication: Rate-splitting multiple access, low-resolution DACs, and RF chain selection," 2022, *arXiv:2202.09128*.

[29] C. Xu, B. Clerckx, S. Chen, Y. Mao, and J. Zhang, "Rate-splitting multiple access for multi-antenna joint radar and communications," *IEEE J. Sel. Topics Signal Process.*, vol. 15, no. 6, pp. 1332–1347, Nov. 2021.

[30] C. Skouroumounis and I. Krikidis, "An evolutionary game for mobile user access mode selection in sub-6 GHz/mmWave cellular networks," *IEEE Trans. Wireless Commun.*, vol. 21, no. 7, pp. 5644–5657, Jul. 2022.

[31] S. Feng, D. Niyato, X. Lu, P. Wang, and D. I. Kim, "Dynamic model for network selection in next generation HetNets with memory-affecting rational users," *IEEE Trans. Mobile Comput.*, vol. 20, no. 4, pp. 1365–1379, Apr. 2021.

[32] D. Tian, J. Zhou, Y. Wang, Z. Sheng, X. Duan, and V.C. M. Leung, "Channel access optimization with adaptive congestion pricing for cognitive vehicular networks: An evolutionary game approach," *IEEE Trans. Mobile Comput.*, vol. 19, no. 4, pp. 803–820, Apr. 2020.

[33] K. Zhu, D. Niyato, P. Wang, and Z. Han, "Dynamic spectrum leasing and service selection in spectrum secondary market of cognitive radio networks," *IEEE Trans. Wireless Commun.*, vol. 11, no. 3, pp. 1136–1145, Mar. 2012.

[34] Y. Han et al., "A dynamic hierarchical framework for IoT-assisted digital twin synchronization in the metaverse," *IEEE Internet Things J.*, vol. 10, no. 1, pp. 268–284, Jan. 2023.

[35] S. Yan, M. Peng, M. A. Abana, and W. Wang, "An evolutionary game for user access mode selection in fog radio access networks," *IEEE Access*, vol. 5, pp. 2200–2210, 2017.

[36] Techplayon. *5G NR Resource Block Definition and RBs Calculation*. Accessed: Apr. 24, 2019. [Online]. Available: https://www.techplayon.com/nr-resource-block-definition-and-rbs-calculation/

[37] H. Xia, Y. Mao, X. Zhou, B. Clerckx, S. Han, and C. Li, "Secure beamforming design for rate-splitting multiple access in multi-antenna broadcast channel with confidential messages," 2022, *arXiv:2202.07328*.

[38] V.-D. Nguyen, T. Q. Duong, H. D. Tuan, O.-S. Shin, and H. V. Poor, "Spectral and energy efficiencies in full-duplex wireless information and power transfer," *IEEE Trans. Commun.*, vol. 65, no. 5, pp. 2220–2233, May 2017.

[39] A. Beck, A. Ben-Tal, and L. Tetruashvili, "A sequential parametric convex approximation method with applications to nonconvex truss topology design problems," *J. Global Optim.*, vol. 47, no. 1, pp. 29–51, Jul. 2010.

[40] A. Ben-Tal and A. Nemirovski, *Lectures on Modern Convex Optimization*. Philadelphia: MPS-SIAM Series on Optimization, SIAM, 2001.

[41] D. Gutermuth. *Picard's Existence and Uniqueness Theorem*. Notes of Fundamental of Differential Equations. Accessed: 2013. [Online]. Available: https://embedded.eecs.berkeley.edu/eecsx44/lectures7Spring2013/Picard.pdf

[42] K. Ciesielski, "On Stefan Banach and some of his results," *Banach J. Math. Anal.*, vol. 1, no. 1, pp. 1–10, 2007.

[43] V.V. Tarasova and V.E. Tarasov, "Concept of dynamic memory in economics," *Commun. Nonlinear Sci. Numer. Simul.*, vol. 55, pp. 127–145, Feb. 2018.
[44] V.V. Tarasova and V.E. Tarasov, "Logistic map with memory from economic model," *Chaos, Solitons Fractals*, vol. 95, pp. 84–91, Feb. 2017.
[45] I. Podlubny, "Fractional differential equations," *Math. Sci. Eng.*, vol. 198, pp. 41–119, Jan. 1999.
[46] H. Tuy, *Convex Analysis and Global Optimization*. Norwell, MA, USA: Kluwer, 2001.
[47] V.D. Nguyen, H. D. Tuan, T. Q. Duong, H. V. Poor, and O.-S. Shin, "Precoder design for signal superposition in MIMO-NOMA multicell networks," *IEEE J. Sel. Areas Commun.*, vol. 35, no. 12, pp. 2681–2695, Dec. 2017.

Nguyen Thi Thanh Van received the B.S. degree from the Hanoi University of Industry, Hanoi, Vietnam, in 2010, and the M.S. degree from Le Quy Don Technical University, Hanoi, in 2014. Her current research interests include robotics, game theory, machine learning, and optimization techniques in communication networks.

Nguyen Cong Luong received the M.S. degree in electronic and telecommunication engineering from the Hanoi University of Science and Technology (HUST). His research interests include the next generation networks.

Shaohan Feng received the B.S. degree from the School of Mathematics and Systems Science, Beihang University, Beijing, China, in 2014, the M.S. degree from the School of Mathematical Sciences, Zhejiang University, Hangzhou, China, in 2016, and the Ph.D. degree from the School of Computer Science and Engineering, Nanyang Technological University, Singapore, in 2020. Since 2020, he works as a Research Scientist with the Institute for Infocomm Research, Singapore. His current research interests include resource management in cloud computing and communication networks.

Van-Dinh Nguyen (Member, IEEE) received the B.E. degree in electrical engineering from the Ho Chi Minh City University of Technology, Vietnam, in 2012, and the M.E. and Ph.D. degrees in electronic engineering from Soongsil University, Seoul, South Korea, in 2015 and 2018, respectively. Since 2022, he has been an Assistant Professor with VinUniversity, Vietnam. He was a Research Associate with SnT, University of Luxembourg, a Post-Doctoral Researcher and a Lecturer with Soongsil University, a Post-Doctoral Visiting Scholar with the University of Technology Sydney, and the Ph.D. Visiting Scholar with Queen's University Belfast, U.K. His current research activity is focused on the mathematical modeling of 5G/6G cellular networks, edge/fog computing, and AI/ML solutions for wireless communications.

He received several best conference paper awards, the Exemplary Editor Award of IEEE COMMUNICATIONS LETTERS in 2019, the IEEE TRANSACTIONS ON COMMUNICATIONS Exemplary Reviewer in 2018, and the IEEE GLOBECOM Student Travel Grant Award in 2017. He has authored or coauthored 60 papers published in international journals and conference proceedings. He has served as a reviewer for many top-tier international journals on wireless communications. He was a technical programme committee member for several flag-ship international conferences in the related fields. He is an Editor for the IEEE OPEN JOURNAL OF THE COMMUNICATIONS SOCIETY and IEEE COMMUNICATIONS LETTERS.

Dong In Kim (Fellow, IEEE) received the Ph.D. degree in electrical engineering from the University of Southern California, Los Angeles, CA, USA, in 1990. He was a Tenured Professor with the School of Engineering Science, Simon Fraser University, Burnaby, BC, Canada. Since 2007, he has been an SKKU-Fellowship and then a Distinguished Professor with the College of Information and Communication Engineering, Sungkyunkwan University (SKKU), Suwon, South Korea. He is a fellow of the Korean Academy of Science and Technology and a member of the National Academy of Engineering of Korea. He has been a first recipient of the NRF of Korea Engineering Research Center in Wireless Communications for RF Energy Harvesting since 2014. He was the General Chair for IEEE ICC 2022 in Seoul. He was selected the 2019 recipient of the IEEE Communications Society Joseph LoCicero Award for Exemplary Service to Publications. He has been listed as a 2020/2022 Highly Cited Researcher by Clarivate Analytics. Since 2001, he has been serving as an Editor, the Editor-at-Large, and an Area Editor for Wireless Communications—I for the IEEE TRANSACTIONS ON COMMUNICATIONS. From 2002 to 2011, he also served as an Editor and a Founding Area Editor of Cross-Layer Design and Optimization for the IEEE TRANSACTIONS ON WIRELESS COMMUNICATIONS. From 2008 to 2011, he served as the Co-Editor-in-Chief for the IEEE/KICS JOURNAL OF COMMUNICATIONS AND NETWORKS. He served as the Founding Editor-in-Chief for the IEEE WIRELESS COMMUNICATIONS LETTERS, from 2012 to 2015.